Generation of Functional Hepatocyte-Like Cells (HLCs) from Human Adipose-Derived Stem Cells (ADSCs) in 2D and 3D

by

Beryl Ngabirano Arinda

Department of Biomedical Engineering
Duke University

Date:_____

Approved:

_____
Jennifer L. West, Supervisor

_____
William M. Reichert

_____
Joel H. Collier

_____
Robert T. Ssekitoleko

Dissertation submitted in partial fulfillment of
the requirements for the degree of Master of Science in the
Department of Biomedical Engineering in the
Graduate School of Duke University

2019

ABSTRACT

Generation of Functional Hepatocyte-Like Cells (HLCs) from Human Adipose-Derived Stem Cells (ADSCs) in 2D and 3D

by

Beryl Ngabirano Arinda

Department of Biomedical Engineering
Duke University

Date:_____
Approved:

_____
Jennifer L. West, Supervisor

_____
William M. Reichert

_____
Joel H. Collier

_____
Robert T. Ssekitoleko

An abstract of a dissertation submitted in partial fulfillment of the requirements for the degree of Master of Science in the Department of Biomedical Engineering in the Graduate School of Duke University

2019

Abstract

Mortality and morbidity rates caused by acute liver failure (ALF), acute-on-chronic liver failure (ACLF) and chronic liver disease continue to rise because of drug induced failure or viral hepatitis, currently with 2,000 cases annually in the United States. Liver transplantation is the only intervention that has shown the most promising patient outcomes, but this approach has major shortcomings like shortage of donor livers, lifelong immunosuppression and a risk of organ rejection after transplantation. Additionally, with rapid liver deterioration and subsequent multi-organ failure characterized by ALF and ACLF conditions, there are high mortality rates as patients await a liver transplant or wait for their livers to regenerate. As such, bioartificial liver support devices provide an alternative to improve patient survival through either offloading liver functions to allow for liver regeneration or by allowing the patient time to receive a liver transplant. These bioartificial liver support devices are designed to perform essential liver functions through incorporation of an active cellular component that performs the liver functions and their success is therefore heavily reliant on the performance of the incorporated cell lines. Because of this, limited sources of these characteristic cell lines with hepatic function is a great challenge being faced in the research and development of the devices.

Adipose-derived stem cells (ADSCs) are a great candidate as a stem cell source for differentiation of hepatocyte-like cells because they can be easily obtained in large quantities with little donor site morbidity or discomfort and have been successfully differentiated into multiple cell lineages. In this study, we investigate the possibility of differentiating human ADSCs into functional hepatocyte-like cells. Furthermore, we investigated the ability to differentiate ADSCs into hepatocyte-like cells in both 2D and 3D environments. We found that induced ADSCs can produce high levels of some hepatocyte functions, like albumin secretion. However, other functions, like urea secretion and cytochrome P450 metabolic activity, while present, are not yet at sufficient levels to be comparable to primary hepatocytes.

Dedication

My mother, inspiration, rock and best friend Ms. Rosemary Bareebe.

Contents

List of Tables

List of Figures

Acknowledgements

My mentor and advisor Dr Jennifer West who graciously gave me the opportunity to learn from her and be a part of her lab for the past year and a half. My mentor Asli Unal, who has had the patience to teach, mentor and advise me during my master's journey. My lab mates that have been great to work with and learn from.

My beloved friends: Lisa Wanda, Emmanuel Opolot, Sandra Batakana, Charlene Chabata, Jovita Byemerwa, Nadia Abutaleb, Dan Kronstad and all my friends that have been a constant support. Catherine Namayega, Martha Tusabe and Jesca Nantume whose friendship, love and support has transcended distance and time.

Dr. Robert Ssekitoleko who has always pushed and encouraged me to do my best. Dr. William Reichert and the Duke-Makerere partnership without whose financial support, I would not have the opportunity to be at Duke University. Beverly Gedvillas who made my transition and stay in the Duke BME program memorable.

My beloved family, who, though miles away in Uganda and all over the world, have supported me with their love and prayers.

Above all, God, through whom I live and breathe and have my being.

1. Introduction

1.1 Background

The liver is a vital body organ that is responsible for over 500 functions. The liver receives 30% of the total circulating blood in a human being per minute and plays a crucial role in physiological regulatory processes in the body [1]. One of the liver's key functions is detoxifying substances that are potentially harmful to the body, like alcohol and drugs.

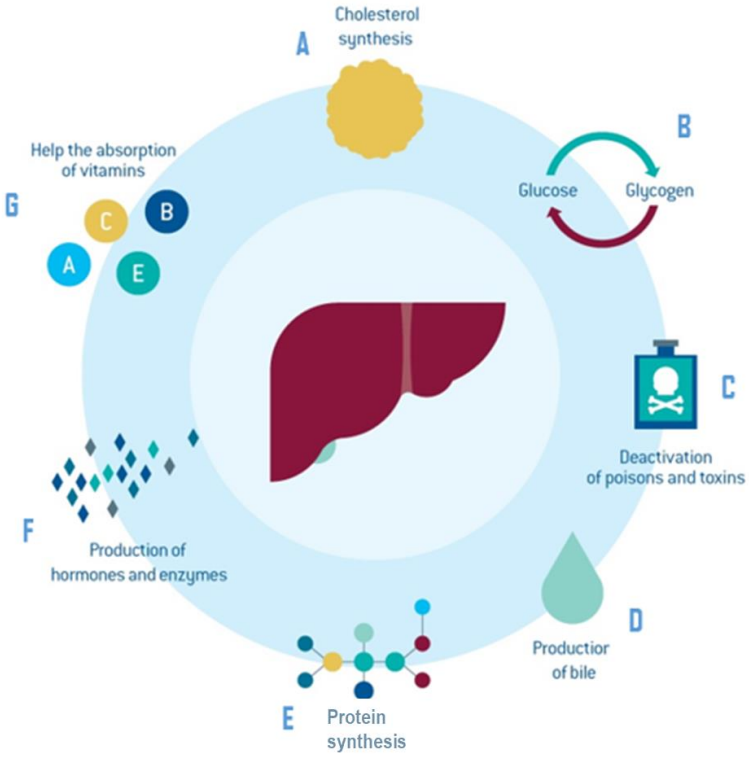

Figure 1.1: A highlight of seven of the liver's main functions. Image adapted from a research paper published by Lonza [2] a) cholesterol synthesis b) metabolism c) detoxification d) bile production e) protein synthesis f) hormone and enzyme synthesis g) absorption of vitamins.

In addition, it also processes and excretes the toxic by-products of normal metabolism, like ammonia or excess hormones [3, 4]. This is especially important for patients undergoing treatment for liver disease, since the liver is responsible for detoxification of drugs meant to help with its very own recovery.

The liver is comprised of different cell types that enable it to perform its functions, such as hepatocytes, sinusoidal endothelial cells, phagocytic Kuppfer cells, and pericyte-like stellate cells [3]. Of the cells comprising the liver, hepatocytes make up 80% of the liver's mass and are responsible for performing majority of the liver's tasks. They are structurally polygonal, organized in palates separated by sinusoidal cells and have an average life of approximately 5 months. The hepatocytes are responsible for protein synthesis of serum albumin, fibrinogen and clotting factors. These cells are therefore the ones most affected in liver disease [5] and are also responsible for the liver's ability to regenerate. The process of liver regeneration is associated with cellular signaling cascades involving growth factors, cytokines, matrix remodeling, and several feedbacks of stimulation and inhibition of growth-related signals [6]. During this process, the liver is able to restore lost mass by proliferation of mature adult hepatocytes and other hepatic cell types as well as restore lost liver functionality [6]. Consequently, techniques or approaches that improve or restore hepatocyte function improve liver function and patient outcomes are being explored such as whole liver transplants [7, 8], partial transplants[7, 9] , hepatocyte transplants [10] and liver support devices [11, 12].

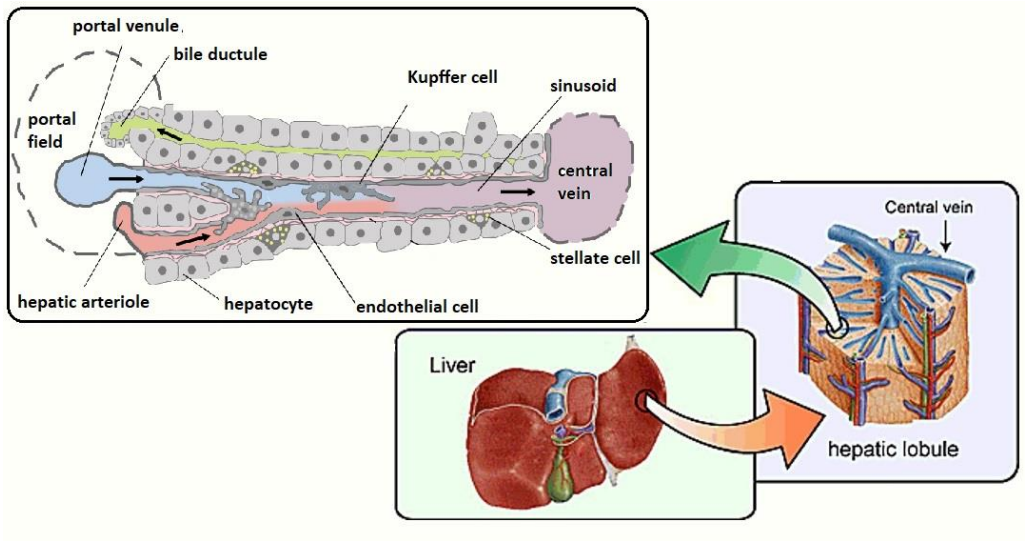

Figure 1.2: Image showing a cross section of liver lobule. It shows the and relative location and distribution of different liver cell types [13]. Hepatocytes, the liver's parenchymal cell type, comprises approximately 70% of the liver's mass. The non-parenchymal cell types including Kupffer cells, stellate cells and sinusoidal endothelial cells comprise approximately 6% of the liver's mass [13].

1.2 Motivation

1.2.1 Problem statement

End stage liver disease (i.e. chronic liver failure) has a high mortality rate and is responsible for approximately 2% of all deaths worldwide. There are several disorders responsible for liver failure including hepatitis, liver tumors, cirrhosis or autoimmune diseases. Cirrhosis of the liver, the replacement of damaged hepatocytes with fibrotic tissue [14], is the most common form of end stage liver disease. Hepatitis, the inflammation of the liver, is a leading cause of cirrhosis [14]. The majority of hepatitis arises from viral infection, but can also arise from autoimmune disorders and drug and alcohol toxicity [14]. Globally, 57% of cirrhosis is attributable to infection either by

hepatitis B (30%) or hepatitis C virus (27%), while 20% of the cases are attributed to alcohol consumption [14]. In 2015, the United States of America alone faced 2.8 million cirrhosis cases and 1.3 million subsequent deaths [15].

Acute liver failure (ALF) has high mortality and morbidity rate due to rapid deterioration of liver function due to the sudden loss of hepatic function without preexisting liver disease [16, 17]. ALF usually results in fast deterioration of liver function due to severe injury of hepatocytes or necrosis processed by multiorgan failure set into motion by loss of hepatocyte function [18, 19]. Globally, the most common causes of ALF are viral hepatitis and drug-induced hepatitis. However, the etiologies vary in developed countries compared to developing countries with hepatitis A, B, and E being the leading causes worldwide [20, 21] and most significantly in developing countries compared to drug-induced liver injury in developed countries [16]. In the United States, drug induced hepatitis accounts for 50% of ALF cases with 2000 cases reported per year according to a report published in 2003 and the numbers continue to increase annually [17]. Acetaminophen hepatoxicity is the most common cause of drug induced hepatitis accounting for 40% of the drug induced ALF cases while idiosyncratic drugs account for the remaining 10% [17, 22]. 20% of all ALF cases are due to unknown causes whereas the remaining cases are attributed to other causes like viral hepatitis, autoimmune liver disease and shock or hypoperfusion [18, 23]. Presently, standard treatment of ALF is supportive care to bridge patients to either transplantation or liver

regeneration and recovery. However, deterioration of patients is relatively fast, and patients become critical in a short period of time leading to death if they do not recover or receive a transplant [24].

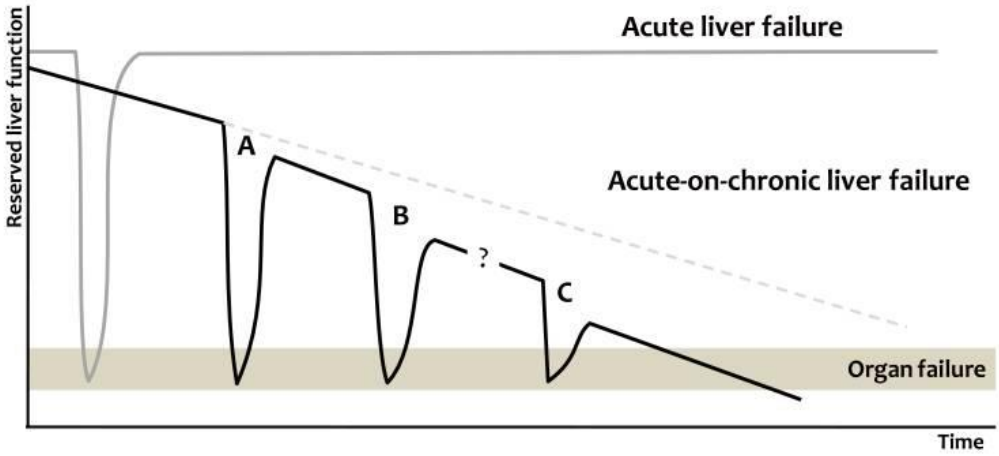

Figure 1.3: The image shown the course of patient deterioration with liver failure. Acute liver failure (grey line), acute-on-chronic liver failure (black line) and liver cirrhosis/chronic liver disease without precipitating insults as adapted from Kim T.Y and Kim D. J. (2013) [25].

Liver failure can also occur due to Acute on-chronic-liver failure (ACLF) which occurs due to a known underlying liver conditions like acute alcoholic hepatitis, acute viral hepatitis or drug induced injuries [26, 27]. ACLF like ALF has a high short-term mortality rate [25, 28]. The image above shows the deterioration of liver function in patients with acute liver failure, acute-on-chronic liver failure, and chronic liver failure. Despite the liver's ability to regenerate, after acute liver failure (ALF) or ACLF, a critical mass of hepatocytes is destroyed thereby resulting in rapid liver deterioration and a cascade of multiorgan failure. In this situation, rapid interventions are required for patient survival.

1.3 Current Interventions

There is a desperate search for interventions to manage liver disease and reduce the mortality rate. Some of the current interventions include liver transplants, stem cell therapies like hepatocyte transplantation, and liver support devices.

1.3.1 Liver transplantation

Liver transplantation remains the most effective treatment for patients with liver failure or end stage liver disease, with continued improvement in survival of patients after transplantation [9]. Unfortunately, liver transplantation is limited by shortage of organ donors, demand for lifelong immunosuppression, and high cost [4, 8]. According to the American Society of Transplant Surgeons 2014 report, increase in the number of patients dying before receiving a liver transplant due to shortage of liver donors [4]. Some patients are removed from the waitlist because of deteriorating health, making them ineligible for a liver transplant. The report showed that in 2014 [4], 1821 patients died while on the waitlist for liver transplant and 1290 were removed from the waitlist because they were too sick to receive a transplant as shown in the table below [4].

Table 1.1: Table showing showing adult transplant waitlist patients from 2012-2014. This includes those removed from the waitlist and reasons why they were removed from the waitlist [4].

	2012	2013	2014
Patients at start of year	15,340	15,130	15,007
Patients added during year	10,184	10,504	10,648
Patients removed during year	10,385	10,598	11,023
Patients at end of year	15,139	15,036	14,632
Removal reason			
Deceased donor transplant	5,463	5,652	5,892
Living donor transplant	192	209	226
Patient died	1,764	1,780	1,821
Patient refused transplant	86	80	104
Improved, transplant not needed	661	588	692
Too sick for transplant	1,176	1,219	1,290
Other	1,043	1,070	998

Liver transplants have been shown to be the approach with the most successful outcomes for both chronic and acute liver disease patients. Donor livers can either be harvested from donors after death or partial liver lobes harvested from living donors. Despite the success of this approach in averting death, the number of patients needing transplants far outnumber the available donor organs. Patients will often die before receiving an organ donation or be too sick to receive one by the time it becomes available. Additionally, there is a risk of organ rejection by the recipient and they must take immunosuppressant drugs the rest of their lives.

1.3.2 Hepatocyte transplantation

Another intervention being explored is hepatocyte transplantation whereby 5-15% of the patient's hepatocytes are replaced by transplanted hepatocytes [10, 29]. The success of this approach is dependent on the functional performance of the transplanted

hepatocytes and their capability to engraft and survive in the host liver [10, 30]. Achieving this has been shown to be a challenge because hepatocytes are harvested from donor livers that have been rejected from transplant patients and therefore there is scarcity of liver tissue for high-quality hepatocyte isolation. There is also a limiting factor in conservation and storage of isolated cells because hepatocytes are known to dedifferentiate and lose function after a few days outside the body [10, 31].

1.3.3 Artificial and bioartificial liver support devices

Due to the limited availability of liver organs and constraints involved in liver transplantation, artificial liver support devices are being explored as a treatment and patient care alternative for ALF and ACLF patients. The devices are meant to temporarily support the diseased liver by filtering and adsorbing accumulated toxins that cannot be cleared by the diseased liver. This is to support regeneration of a patient's liver or to take on liver functions until a liver donor becomes available. There are two types of artificial liver support device: non-biological and bioartificial liver support devices.

Non-biological models of the liver support devices are designed to carry out detoxification through different approaches like plasmapheresis, hemodialysis, plasma exchange, and hemoperfusion [32-34]. The non-biological liver support devices combine mechanical techniques to eliminate both water-solved and albumin bound toxins. The water soluble toxins can be removed by hemodialysis and hemofiltration, while the

albumin bound toxins are removed by either using large pore filters to separate plasma proteins, like in the Prometheus and Selective Plasma Filtration Technology (SEPET) device models or by adding albumin to the dialysate for removal of albumin-bound toxins, like in the Molecular Adsorbent Recirculating System (MARS) and Single Pass Albumin Dialysis (SPAD) devices [35, 36].

Table 1.1: The table below shows a summarized comparison between artificial liver support devices and bioartificial liver support devices [5]

Non-biological liver support devices	**Bioartificial liver support devices**	
	Human cell line	Porcine hepatocytes
Molecular Adsorbents recirculating system (MARS)	Extracorporeal Liver Assist Device (ELAD)	HepatAssist™
Fractionated plasma separation and adsorption (Prometheus)		Bioartificial Liver support system (BLSS)
Single pass albumin dialysis (SPAD)		Amsterdam Medical Centre Bioartificial Liver (AMC-BAL)
Selective Plasma Filtration therapy (SEPET)		Molecular Extracorporeal Liver Support (MELS)

Even though non-biological artificial liver support devices can successfully eliminate some toxic metabolites from a patient's blood, they cannot perform synthetic and metabolic functions [37]. This is not a sustainable solution since other liver functions are necessary to avoid multiorgan liver failure. Therefore, patients are not able to survive long without a longer-term solution like liver transplant or liver regeneration [1,

5]. Bioartificial liver devices on the other hand are designed to address these shortcomings by addition of cellular component to incorporate certain liver functions like oxidative detoxification, biotransformation, excretion and synthesis [38, 39]. Bioartificial liver support devices function by circulating a patient's plasma over metabolically and functionally active hepatocytes in a bioreactor where the hepatocytes are cultured and induced to perform hepatic functions [37].

The current bioartificial liver support devices include HepatAssist™, Extracorporeal Liver Assist Device (ELAD), Modular Extracorporeal Liver support (MELS), BLSS and AMC-BAL [37, 40]. These devices incorporate the cellular components by either hollow fiber systems or flat membrane sheet systems. While these systems would ideally function best with human primary hepatocytes, their use is limited because of their lack of availability [30]. There are limited sources of primary hepatocytes because healthy donor livers are scarce, and any that are available would rather be used for transplantation instead of harvesting hepatocytes [13]. Consequently, only discarded organs and tissues are available to harvest hepatocytes for use in the bioartificial liver support devices. Furthermore, primary human hepatocytes lose viability because they do not proliferate efficiently and dedifferentiate quickly in vitro. For clinical efficacy, the bioartificial liver support device requires approximately 10^{10} hepatocytes in order to provide even 10% of total liver function [41]. Using primary

human hepatocytes has therefore been largely limited because of the lack of a reliable cell source that generates large cell numbers whilst maintaining metabolic functionality.

Table 1.2: The table below is a comparison of pros and cons between different liver disease interventions. This compares liver transplantation, artificial and bioartificial liver support devices as interventions for liver disease patients based on the discussion above.

Intervention	Pros	Cons
Liver transplant	a. Successful outcome b. Less risk of recurrence	a. Risk of rejection b. Lifetime on immunosuppression medications c. Long waitlist d. Donor shortage
Non-biological support devices	a. Detoxification of blood, therefore less strain on liver b. Simple devices	a. No metabolic or synthetic liver-specific functions b. Not a long-term solution
Bioartificial support devices	a. Metabolic and synthetic liver functions b. Longer patient survival time c. Faster liver regeneration potential	a. Shortage of cell sources for bioactive component b. Short term viability due to cell death and dedifferentiation

1.4 Cell sources for Bioartificial liver support devices

Alternative cells sources used in liver support devices include porcine hepatocytes, tumor-derived and immortalized cell lines, adult and embryonic stem cells and stem cell-derived hepatocyte-like cells [13, 41]. The use of primary hepatocytes from animal sources like pigs has been constrained by potential transmission of zoonotic

diseases, potential immune responses and protein incompatibility. Although tumor-derived sources C3A and HepG2 cell lines have been shown to have great expansion potential, they have limited hepatocyte functionality and have a high risk of tumorigenesis [41].

Stem cells are highly proliferative activity and are multipotent in nature thereby providing a source of hepatocytes by differentiating the stem cells into functional hepatocytes [29, 30]. Stem cells for this purpose can be derived from human embryonic stem cells (hESCs) [13], human induced pluripotent stem cells (iPSCs) [13, 42], human liver progenitor cells (HLPCs) [13, 41], and human mesenchymal stem cells (MSCs) [41] all of which have been shown to possess the potential ability for differentiation of hepatocytes. Human embryonic stem cells however face ethical hurdles for clinical applications while human liver progenitor cells (HLPCs) can only be harvested from either fetal liver or healthy adult liver tissue and therefore have limited sources [13, 37]. On the other hand, a promising alternative that overcomes many of the above-mentioned limitations are adult derived stems cells, which have high proliferative potential and are multipotent, making them a scalable source [43].

Potential sources being explored for adult derived stem cells are induced pluripotent stem cells which are reprogrammed somatic cells. Research has shown that fully differentiated adult cells like fibroblasts or skin cells, could be reprogrammed to an undifferentiated, pluripotent state similar to embryonic stem cells through the forced

expression of reprogramming factors. These form induced pluripotent stem (iPS) cells that have self-renewal capabilities and pluripotent differentiation potential thereby being a candidate since they can be sourced from adult somatic cells [42]. The limitation to using this is being able to generate the large quantities of cells required for use in bioartificial liver support devices [13, 44].

Similarly, Mesenchymal Stem Cells (MSCs) [45] can be derived from adult human tissue like the bone marrow, adipose tissue, peripheral blood, muscle, synovial membrane. Even though bone marrow derived MSCs have shown great differentiation potential into hepatocyte-like cells, harvesting enough bone marrow to acquire the number of cells required is invasive and complicated. On the other hand, MSCs derived from adipose tissue have been shown to share similar differentiation potential into hepatocytes [46]. Adipose-derived stem cells can additionally be obtained in large quantities through a minimally invasive liposuction procedure. Large quantities of lipoaspirate obtained from liposuction procedures can be used to obtain several million Adipose-derived Stem Cells (ADSCs), and the successful differentiation of human ADSCs to hepatocytes would bridge this gap in the search of cell sources, as they would be the most abundantly available and accessible source.

In pursuit of a reliable and efficient cell source for viable hepatocytes, research into the differentiation of ADSCs into hepatocytes show promise of an abundant and reliable cell source. Unlike mesenchymal stem cells, that are derived from other sources

like the bone marrow, ADSCs can be easily and repeatably harvested using minimally invasive techniques, like liposuction, with low morbidity. They can be found in any type of white adipose tissue, including subcutaneous and omental fat [47]. With an increase in the number of patients undergoing elective liposuction in the western world, lipoaspirate, which would normally be discarded as medical waste, is an ideal source of ADSCs. The liposuction procedure has a complication rate of around 0.1% and therefore causes minimal risks to the donor [47]. Research also shows that approximately 16 x 108 cells ADSC cells can be obtained per 120 mL lipoaspirate with 98–100% of the adipose cells in the lipoaspirate viable, making this a favorable alternative cell source [47]. Furthermore, ADSCs are multipotent and have the capacity to differentiate into various cell types including osteocytes, vascular endothelial cells, pancreatic β-cells, and hepatocytes. They also have immunosuppressive properties and low immunogenicity therefore decreasing the risk of rejection [46].

Table 1.3: Comparison of different cell sources potentially used in bioartificial liver support devices to incorporate hepatocyte-like functions. Adapted and modified from Kelly S. et al. [13]

Cell Source		Pros	Cons
Primary hepatocytes	Human adult and fetal	• Ideal hepatocyte function	• Limited sources large enough quantities • Limited expansion potential • Phenotypic instability

	Xenogeneic (Porcine)	• Large quantities can be obtained	• Immunogenicity • Xenozoonotic • No human protein synthesis
Immortalized hepatocyte lines	Tumor-derived & Gene transfer cells (SV40, telomerase)	• Good expansion potential	• Limited range of functions • Genomic instability • Tumorigenicity
Stem Cells differentiated into Hepatocyte-like cells (HLCs)	Human embryonic stem cells (hESCs)	• Good differentiation and expansion potential • Potentially good hepatocyte-like function	• Ethical limitations in clinical applications • Differentiation efficiency • Phenotypic instability • Limited sources large enough quantities
	Human liver progenitor cells (HLPCs) (hepatoblasts, oval cells)	• Good hepatocyte-like function • Good differentiation efficiency	• Limited sources for large enough quantities
	Human Induced pluripotent stem cells (iPSCs)	• Good hepatocyte-like function	• Differentiation efficiency • Phenotypic instability • Limited expansion potential
	Adipose-derived stem cells	• Good hepatocyte function • Low immunogenicity	• Differentiation efficiency • Phenotypic instability

		• Large quantities can be obtained relatively easily	
	Other Mesenchymal Stem Cells (MSCs) like bone marrow derived MSCs	• Good hepatocyte-like function	• Differentiation efficiency • Phenotypic instability • Limited sources for large enough quantities

1.5 Design rationale

In the treatment of acute and acute-on-chronic liver failure, successful liver transplantation is the only therapy that has shown effective patient outcomes [21]. Nonetheless, the number of patients requiring liver transplants is increasing and the demand far outweighs the available donor livers. Subsequently, liver support devices have been employed to support patients while their liver recovers or while they are waiting for a transplant [36]. An ideally effective bioartificial device would therefore need to be able carry out the main functions of the liver including detoxification and biosynthesis [37]. To achieve this, current bioartificial liver support devices use hepatic cell lines derived from various sources like porcine hepatocytes, tumor cell lines or harvested from donor livers which are unsuitable for transplant [41]. Unfortunately, these sources all have severe shortcomings [39]. Few functional hepatocytes can be

harvested from diseased livers, and porcine and tumor cell lines pose a risk of infection or malignancy transmission. A reliable and scalable source of 'ideal' cells in these bioartificial liver support devices therefore continues to be a challenge[36].

Adipose-derived stem cells (ADSCs), however, are easily obtained in large quantities with little donor site morbidity or discomfort [47]. As such, they have been explored as a stem cell source for a variety of applications, including forming human hepatocyte-like cells. The ability to generate hepatocyte-like cells from human ADSCs would greatly increase the amounts of functional hepatocytes available for use in these devices as well as in research.

1.6 Hypothesis and study aims

The focus of this research is to generate functional hepatocyte-like cells (HLCs) by differentiating human ADSCs. A study carried out by Xu et al. in 2015 [48] showed that that with a series of growth factor treatments, rat adipose-derived stem cells were able to differentiate into hepatocyte-like cells with functional hepatocyte properties. The authors were able to show that the hepatocyte-like cells were able to synthesize albumin and urea at quantities comparable to primary hepatocyte cells [48]. This is important because these properties are specific to liver hepatocyte function. They were also able to assess enzymatic activity by testing for cytochrome P450 activity of different cytochrome enzymes as an indicator of drug metabolic activity [48].

Aim 1: Effectively generate functional hepatocyte-like cells from human adipose-derived stem cells cultured in 2D. The goal is to differentiate human ADSCs under specific culture conditions in vitro by referencing the differentiation experiment design developed by Xu et al. (2015). The hepatocyte functions that will were investigated are albumin and urea synthesis and enzyme cytochrome P450 activity.

Aim 2: Optimize differentiation of functional hepatocyte-like cells in 3D. Hepatocyte function is affected by several factors like extracellular signaling molecules, cell-cell interactions, cell-matrix interactions and physical factors. By differentiating the human ADSCs in biofunctionalized poly (ethylene glycol) (PEG) hydrogels, we will be able to investigate and regulate generation of HLCs with hepatocyte specific functions.

2. Studying differentiation of ADSCs to HLCs in 2D

Stem cells can differentiate into different cell types depending on the conditions of their environment. Efficient and rapid differentiation of stem cells is important in order to provide a suitable and reliable source of hepatocytes. As mentioned in chapter 1, ADSCs are a great candidate for hepatic differentiation because large numbers of cells can be harvested minimally invasively. Previous studies showed that rat ADSCs can be induced to differentiate into hepatocyte-like cells (HLC) by treating them with a series of media conditions containing different growth factors like Oncostatin M (OSM), Endodermal Growth Factor (EGF), Hepatocyte Growth Factors (HGF) and Fibroblast Growth Factor 4 (FGF-4). The ADSCs are first induced into definitive endodermal cells and then further induced into hepatogenic progenitor cells. Finally, the hepatogenic progenitor cells are induced into mature HLCs [48]. Consequently, the focus of aim 1 is to differentiate human ADSCs into functional HLCs that can carry out carry out some of the major liver functions like protein synthesis and enzymatic activity

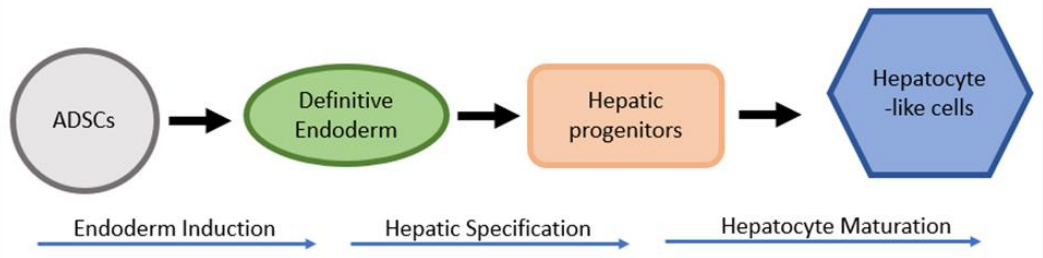

Figure 2.1: The phases of differentiation of induced ADSCs into mature functional HLCs [49, 50]

2.1 Materials and Methods

2.1.1 Cell culture

Human adipose-derived stem cells (Lonza) were cultured using aseptic technique on collagen- coated plates at 37°C and 5% CO_2. At passage 3-4, the cells were seeded on collagen-coated 6-well plates at a density of 5×10^4 cells/cm^2. They were then maintained in Eagle's Essential Medium (Sigma) supplemented with ADSC Growth Medium Bullet Kit (Lonza) containing ADSC basal medium and ADSC-GM SingleQuots™ growth supplements (containing L-Glutamine and Gentamicin sulfate amphotericin -B). At approximately 90-100% cell confluence, the cells were treated with a series of media changes for a period of 9 days as detailed below.

For the first day, ADSCs were maintained in endodermal induction (EI) media comprised of RPMI-1640 (Thermofisher) supplemented with 100 nM Inducer of Definitive Endoderm 1 (IDE1) (Stemcell Technologies) and 3 μM CHIR99021 (Stemcell Technologies). IDE1 induces differentiation of stem cells into definitive endoderm via the Activin/Nodal pathway [40] while CHIR99021 is an aminopyrimidine derivative that is an inhibitory target of GSK3 and a WNT pathway activator [41]. Studies have shown that WNT signaling is required to specify definitive endoderm by regulating SOX17 expression which is vital for endoderm formation [41].

On day 2, for hepatic specification, the culture medium was replaced with hepatogenic induction (HI) medium. HI medium comprised of RPMI-1640 (Thermofisher) containing 100 nM IDE1, 20 ng/mL Fibroblast Growth Factor 4 (FGF-4;

PeproTech) and 150 ng/mL Hepatocyte Growth Factor (HGF; PeproTech). FGF-4 is a heparin binding growth factor [50] and HGF is thought to induce hepatogenic differentiation, morphogenesis and proliferation [50]. The cells were maintained in this media for 3 days with media changes every 48 hr.

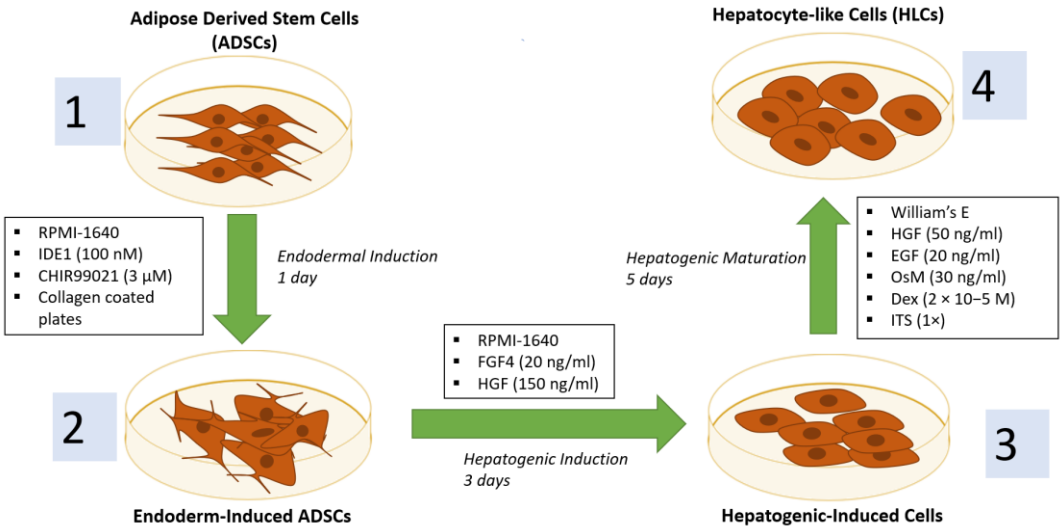

Figure 2.1: Schematic diagram drawn to show the protocol observed for differentiation of ADSCs into HLCs. This protocol was described and carried out by Xu. et al. (2015) and was adapted for this study to differentiate human ADSCs to functional HLCs in 2D culture conditions.

Finally, during the maturation step, the cells were cultured in hepatogenic maturation (HM) media comprised of Williams' E media (Gibco) supplemented with 50 ng/mL HGF, 20 ng/mL Epidermal Growth Factor (EGF; PeproTech), 30 ng/mL, Oncostatin M (OSM; PeproTech), 20µM Dexamethasone (Dex; Sigma) and 1 µl/mL ITS liquid media supplement (containing insulin/transferrin/selenium; Sigma). OSM is a

growth and regulatory factor [50], EGF stimulates proliferation [50] and Dex has been shown to promote maturation of hepatocytes from stem cells [50].

The cells were maintained in this media for 5 days with media changes at 48 hr intervals. All the growth factors were reconstituted 2 hr, no vortexing or centrifuging was done during reconstitution and no media was kept for more than 1 week. Phase images of the cells were taken at the end of every media cycle in order to observe morphological changes using a Zeiss Axiovert 135 inverted microscope.

2.1.2 Immunohistochemistry staining and confocal imaging

For intracellular staining, the cells were fixed with 8% paraformaldehyde for 20 min and then rinsed three times with 1× PBS for 5 min each. The cells were then permeabilized by incubating them with PBS containing 0.125% Triton X-100 (Sigma) for 10 min and then washed four times with PBS. After blocking with 3% donkey serum in PBS for 1 hr, the cells were incubated with primary antibodies (described below) diluted in PBS containing 0.05% donkey serum for 2 hr. These were all performed on a rocker at room temperature.

The cell markers selected were: albumin because albumin secretion is a key functional property of mature hepatocytes; CD90 because this is a marker of ADSCs and this marker would indicated if the ADSCs differentiated to another cell type or if they maintained ADSC markers; and anti-hepatocyte nuclear factor alpha-3 (anti-HNF3β) which is also a mature hepatocyte marker. The primary antibodies used in the study

were goat anti-ALB (1:150; Bethyl), mouse anti-CD90 (1:200; Biolegend), and rabbit anti-hepatocyte nuclear factor alpha-3 (anti-HNF3β, 1:300; Cell Signaling).

After this stage, the cells were then rinsed three times for 2 hr in PBS with 0.01% Tween20 for the first three washes and the fourth wash with PBS without Tween20. They were then incubated with the appropriate corresponding fluorescently-conjugated secondary antibody diluted in PBS + 0.05% donkey serum according to the respective dilution ratios below. The samples were then left overnight on a rocker at 4^0C in the dark. The corresponding secondary antibodies used were Alexa Fluor 488 conjugated donkey anti-rabbit IgG (1:200, Thermofisher), Alexa Fluor 555 conjugated donkey anti-mouse IgG (1:200, Thermofisher), Alexa Fluor 647 conjugated donkey anti-goat IgG (1:200, Thermofisher).

Cells were then washed with PBS and nuclei were stained by incubation with 4',6-diamidino-2-phenylindole (DAPI, Sigma) for 2 hr and washed 3 times for 10 min each with PBS. The samples were then imaged using a Zeiss LSM 880 inverted confocal airyscan microscope. Images were taken at 20x objective, 1024 x 1024 pixels. The images were then compiled using Image J software.

2.1.3 Hepatic Functional Assays

In order to investigate the properties of the HLCs differentiated from the human ADSCs, carried out assays to determine albumin production and cytochrome P450 (3A4) enzymatic activity. The same assays were also carried out on human primary

hepatocytes cultured on collagen coated plates as well as on undifferentiated human ADSCs for our controls.

2.1.3.1 Albumin Assay

Albumin synthesis is one of the major properties of mature hepatocytes and an albumin assay was carried out to determine if the differentiated HLCs were producing albumin. The ELISA Quantification and starter kit used during this assay were products of Bethyl Laboratories Inc. We started by coating the transparent 96-well microtiter plate with 1 μl of affinity purified antibody diluted with 100 μl of coating buffer (carbonate-bicarbonate solution) for each well. The plate was then incubated at room temperature for 1 hr in 100 μl of the 0.1 μl/mL diluted antibody. After incubation and aspiration of the antibody solution, the plate was washed 5 times using ELISA wash solution (50 mM Tris buffered saline, pH 8.0, 0.05% Tween20, Sigma). 200 μl of blocking solution (50 mM Tris buffered saline, pH 8.0, 0.1% bovine serum albumin, Sigma) was then added and to each well and incubated got 30 min before washing five times with ELISA wash solution.

The next step was to add 100 μl of prepared standard and sample solution to each well before incubating for 1 hr. The standard concentrations used were 400 ng/mL, 200 ng/mL, 100 ng/ mL, 50 ng/mL, 25 ng/mL, 12 ng/mL, 6.25 ng/mL and 0 ng/mL diluted using conjugate diluent solution. The standards and sample solutions were added in triplicates per sample into the wells. The wells were then washed five times before

adding 100 µl of HRP detection antibody diluted to a ratio of 1:75,000 using conjugate diluent. After incubation for 1 hr and washing again 5 times, 100 µl of TMB substrate solution was then added to each well and left in the dark to incubate for 15 min. The reaction was then stopped with 100 µl of stop solution (0.18 M H_2SO_4) added to each well. The absorbance of each well was then measured on a plate reader at 450 nm.

2.1.3.2 Cytochrome P450 (3A4) assay

Cytochrome activity in hepatocytes is important for drug metabolism, an important role of hepatocytes. This is therefore an indicator of hepatocyte function of HLCs [48]. In this study, CYP3A4 activity was investigated. The cells were treated with 25 mM Rifampin diluted in HM media for 72 hr with a media change after 24 hr. After this, proluciferin-conjugated substrate was added and incubated at 37^0C and 5% CO_2 for 1 hr. The proluciferin-conjugated substrate used was 3 µM Luciferin-IPA. Both culture medium collected from the wells with cells and Luciferin detection reagent (LDT) were transferred to a white opaque 96-well luminometer plate with a 1:1 ratio in each well (100 µl sample: 100 µl LDT) for 20 min after which the fluorescence was then measured by a plate reader. The fluorescence was then measured, and this was used to determine to calculate the concentration of produced of CYP generated D-luciferin. This is directly proportional to the CYP450 (3A4) enzymatic activity present in the cells.

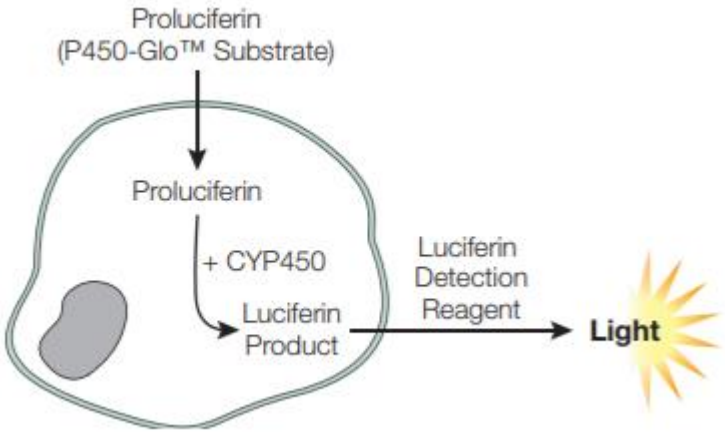

Figure 2.2: Schematic showing the principle of the cell-based P450 (3A4) assay used in the experiment. A proluciferin substrate (Luciferin-IPA) enters cells from the culture medium and the CYP450 enzyme cleaves the proluciferin releasing luciferin which is then detected with Luciferin Detection Reagent (LDR). The image is adapted from the P450-Glo™ Assay protocol.

3. Differentiating human ADSCs in 3D environment

Cells have been observed to behave differently in 2D culture compared to 3D culture environments [51] . The behavior in 3D environments is believed to more closely mimic the cell behavior in vivo. 3D culture offers spatial configuration like the complex architecture in which cells exist while in the body. The way cells interact in the 3D microenvironment affects a range of cellular functions like proliferation, differentiation, morphology, protein expression, and responses to external stimuli [52]. Hydrogels are often used to provide the three-dimensional culture environment for soft tissue-like properties in tissue engineering applications [53].

Hydrogels used in tissue engineering can be categorized as natural or synthetic based on their composition. Natural hydrogels are derived from biological sources such as collagen, fibrin chitosan and alginate [54, 55]. They are naturally biologically active but also have batch-to batch differences that makes it difficult to reproduce experiments due to limited control over mechanical properties. Artificial hydrogels on the other hand have a uniform defined structure and therefore offer more control of desired properties like viscoelasticity. Some synthetic hydrogels include poly (ethylene glycol) (PEG), poly (vinyl alcohol) (PVA) and poly (N-isopropylacrylamide) (PNIPAAm) [51, 55]. These synthetic hydrogels have no inherent biological activity but allow tunability of certain properties such as degradation, stiffness, elasticity and cell-specific bioactivity. For purposes of this research study, we used a bioactive PEG-based hydrogel.

As mentioned in the previous chapter, Xu et al. were able to induce differentiation of rat ADSCs in 2D culture into HLCs. Based on this paper and using the same protocol, we proceeded to induce differentiation of human ADSCs in 2D culture into HLCs. In order to observe the behavior of cells in a 3D environment that more closely represents in vivo environment, we encapsulated ADSCs in a bio-actively modified PEG-based hydrogel.

3.1 PEG hydrogels

Poly (ethylene glycol) is a hydrophilic polymer that is approved by the FDA for biomedical applications and has been widely used for tissue engineering application [56]. This hydrogel acts as "blank slate" because its hydrophilic nature makes it resistant to protein adsorption. The properties of the hydrogel can be modified by altering the PEG molecular weight, concentration, and functionality [51, 54]. It is therefore our polymer of choice because of its tunable properties. It also has a poly(ether) backbone which is hydrolytically stable and serves as a biostable platform [57].

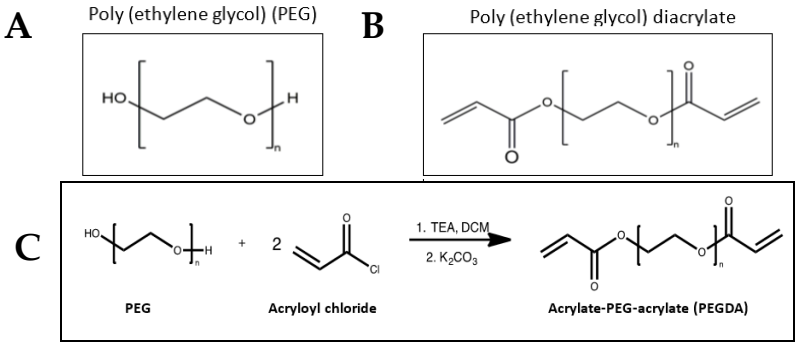

Figure 3.1: Chemical structures of PEG and PEGDA. A) PEG and B) PEGDA respectively and C) shows chemical reaction involved in PEGDA.

During this study, PEG was modified to incorporate terminal acrylate groups forming PEG diacrylate (PEGDA). While forming the hydrogel, the terminal acrylate groups promote crosslinking via free radical-based photopolymerization which is both a rapid and mild reaction [56, 58]. Mild photo crosslinking conditions help to maintain high cell viability during encapsulation. Because we need to have homogenous cell distribution, we mix cells in the hydrogel precursor polymer solution before the crosslinking photopolymerization reaction is initiated [58, 59]. The process of crosslinking should therefore be fast enough to minimally compromise cell viability. The photo initiator system of choice for this study was Eosin Y, because it is biocompatible and stable, and we use triethanolamine (TEOA) as the co-initiator. Upon light exposure, Eosin Y is excited to a triplet state and undergoes a single electron redox reaction with triethanolamine (TEOA) as the electron donor. The generated free radical is propagated by addition of the radicle to the double bonds and causes growth of the polymer chain until termination of the reaction.

3.2 Degradation of PEG hydrogels

In order to mimic extracellular (ECM) conditions in the 3D hydrogels, it is important for the hydrogel to be able to remodel to allow cell migration and proliferation [60]. PEGDA can undergo ester hydrolysis naturally but not fast enough to match the pace required by cells in culture. In order to achieve this property, we added a protease sensitive peptide to the hydrogel backbone which makes the hydrogel

biodegradable in response to cellular Matrix Metalloproteases (MMPs). The peptide used in the study has the sequence, GGGPQG↓IWQGK and is enzymatically degradable by MMP-2 and MMP-9 secreted by the cells [58, 60].

3.2.1 PEG-PQ-PEG Synthesis

This peptide sequence, GGGPQG↓IWQGK, as used for this study, was synthesized by solid phase peptide synthesis based on standard Fmoc chemistry using an Apex 396 peptide synthesizer (Aapptec). To incorporate the bioactive peptide, we form acrylate-PEG-biomolecule by reacting a hetero-bifunctional acrylate PEG to a free amine or terminal carboxyl group on the peptides chain as seen in the figure below. The bioactive peptides are therefore incorporated into the hydrogel matrix during crosslinking.

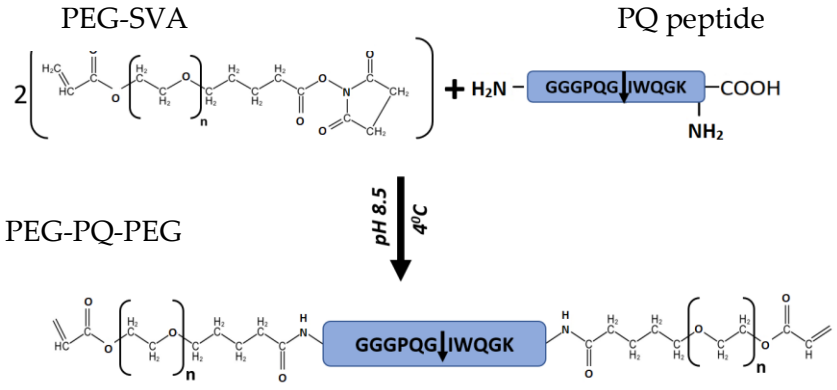

Figure 3.2: Reaction involved in creating biodegradable PEG based hydrogel. This was achieved by incorporation of protease sensitive peptide into polymer backbone in order to make the hydrogel responsive to proteases released by cells thereby mimicking ECM properties in that regard. ↓ indicated in the peptide sequence represents the cleavable site of the peptide

The polyethylene glycol valeric acid (PEG-SVA) to PQ ratio used in the reaction was 2.1:1 maintained at a pH of 8. The PEG chains were conjugated at the N-terminus and the lysine residue at the C-terminus of the peptide to form Acryl-PEG-PQ-PEG-Acryl. Once the pH of the reaction is stabilized at pH 8, it was then kept for 16 hr at 4^0C to allow the reaction to reach completion. The solution was transferred to a 3500 Da MWCO dialysis membrane and dialyzed against 4L ultra-pure water for 20 hr with 4-5 water changes. The resulting solution was then frozen and lyophilized. Conjugation efficiency was then validated by Gel Permeation Chromatography (GPC).

GPC was carried out first by preparing the PEG-SVA and PEG-PQ-PEG samples by dissolving them in 0.1% ammonium acetate in DMF solvent at a concentration of 2 mg/mL. The samples were then pumped through a polystyrene/divinylbenzene matrix (PL gel column, 5 μm porosity, 500 Å pore size, Polymer Laboratories) and analyzed with an evaporative light scattering (ELS) detector. Conjugation success was then determined by the degree of separation between elution peaks of Acryl-PEG-SVA and Acryl-PEG-PQ-PEG samples.

3.2.2 PEG-PQ-PEG Hydrogel formation

Like in PEGDA hydrogel formation described above, PEG-PQ-PEG hydrogel was made by photopolymerization of 2 μl of precursor polymer solution exposed to white light of 150 mW for 35 sec per gel. The PEG-PQ-PEG polymer solution was prepared by dissolving PEG-PQ-PEG peptide prepared in the section above in 10mM HEPES buffer

solution containing 1.5% v/v TEOA (HBS-TEOA). The solution was stored at 20% polymer concentration at -20^{0}C and subsequent dilutions prepared according to required need.

The hydrogel precursor solution contained PEG-PQ-PEG, 3.5 μM/mL N-vinyl pyrrolidone (NVP, sigma) and 10 μM eosin Y. The solution was filtered using a filter with 0.2 μm pores and mixed well to ensure uniformity. 2 μl of the solution was then pipetted onto glass slides made hydrophobic by treatment with Sigmacote (Sigma), between two 380 μm-thick polydimethylsiloxane (PDMS) spacers and covered with a methacrylate-modified cover slip before exposing it to the light source.

Sigmacoted glass slides were used because the surface is hydrophobic so that PEG will not attach to the glass slide surface during photopolymerization. The Sigmacoted slide was prepared by first cleaning microscope glass slide with acetone. The glass slide was then immersed in Sigmacote on a Petri dish for 30 sec and then put on a rack to dry. The slides were then immersed and dried five times and then incubated in an oven until they were completely dry.

The methacrylate-modified cover slips were used to enable adhesion of polymer droplets. 12 mm coverslips were cleaned in solution of 1:1 hydrogen peroxide and sulfuric acid for 1 hr before adding 3-(trimethoxysilyl) propyl methacrylate (2% v/v diluted in ethanol) for 48 hr on a rocker at low speed. The methacrylate-modified

coverslips were then cleaned with ethanol, dried overnight and sterilized under UV light before use.

3.2.2.1 PEG-PQ-PEG degradation study

The degradation properties of the hydrogel were tested by carrying out a collagenase degradation study. This was carried out by incubating PEG-PQ-PEG and PEGDA hydrogels in a collagenase solution from clostridium histolyticum (Sigma) at a concentration of 15 μl/mL with 0.36 mM calcium chloride solution at 37^0C and 5% CO_2. Collagenase recognizes the PQ peptide and thereby degrades the hydrogel. As the hydrogel is being degraded by cleaving the peptide, tryptophan from PEG-PQ is released into the solution and evaluated every hour for degradation until 100% degradation was achieved.

3.2.2.2 PEG-PQ-PEG Compression testing

ADSCs differentiation behavior can be influenced by the mechanical properties of the 3D culture environment and this external influence can affect the differentiation pathway of the hepatocyte-like cells [51]. To determine the mechanical properties of the hydrogels, they were characterized by determining the compressive modulus from compression testing using a Micro-strain analyzer (TA Instruments RSA III). Hydrogels were formed (as described in the PEG-PQ-PEG synthesis section) and left overnight in PBS to allow maximum swelling. The stress-strain data obtained was plotted and the compressive modulus determined from the linear regions of the curve.

3.3 Cell adhesion properties in PEG hydrogels

For this study, the peptide Arginine-Glycine-Aspartic Acid-Serine (abbreviated RGDS) was selected to serve as an integrin binding motif for cells to promote cell adhesion and spreading. This was done by covalently immobilizing crosslinking the peptide into the PEG-hydrogel network using a PEG-monoacrylate linker.

3.3.1 PEG-RGDS synthesis

PEG-RGDS was synthesized similar to PEG-PQ-PEG described above by reacting RGDS peptide with PEG-SVA in 20 mM HEPES buffer solution at a molar ratio of 1.2:1. The solution was then left overnight in order for the reaction to reach completion and then dialyzed using a 3500 Da MWCO dialysis membrane against 4L ultra-pure water for 24 hr with 4-5 water changes in between. The resulting solution was then frozen and lyophilized to dryness for 48 hr. Conjugation efficiency was also shown by GPC as described above.

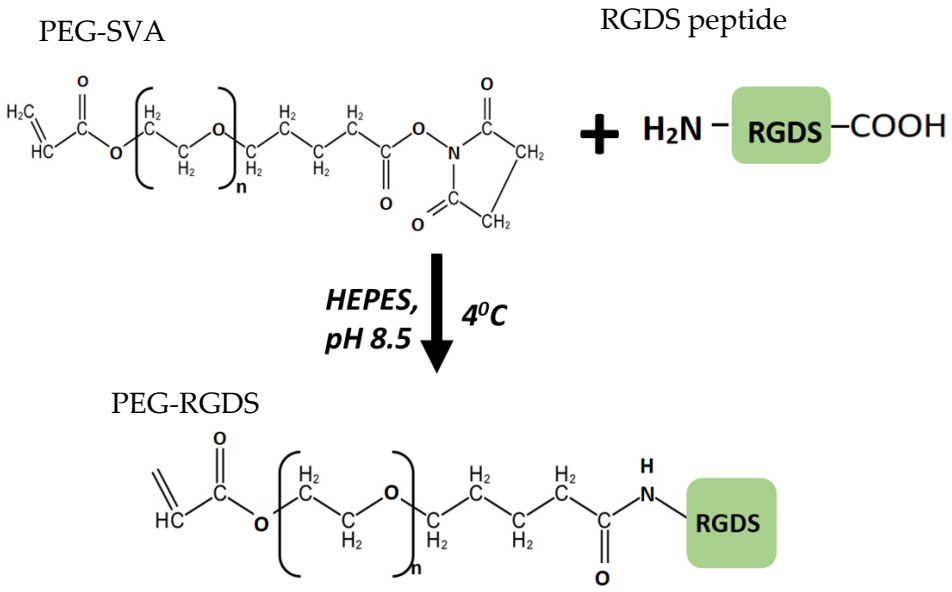

Figure 3.3: Reaction involved in synthesis of PEG-RGDS. RGDS is the cell adhesive peptide we incorporated into the hydrogel to increase hydrogel bioactivity and mimic ECM properties.

3.3.2 PEG-RGDS hydrogel formation

To create hydrogels containing PEG-RGDS, the PEG-RGDS precursor solution was formed by dilution to appropriate concentrations in HBS-TEOA, and hydrogel precursor solution made as described above.

3.3.2.1 Cell adhesion study

The cell adhesion study was performed on the surfaces of PEGDA hydrogels modified crosslinked with PEG-RGDS in order to confirm the bioactivity of the synthesized PEG-RGDS after conjugation. PEGDA was used because unlike PEG-PQ-PEG, there would not be any cell driven degradation of the hydrogel. 5% PEGDA, 3.5mM PEG-RGDS, and photo initiator solution (10 μM eosin Y and 3.5 μM/mL NVP)

were combined and, filtered, and gels formed by photopolymerization as previously described. The gels were left overnight in PBS to allow the hydrogel to swell. Mile Sven 1 (MS1) cells were then seeded onto the hydrogels and observed for cell attachment and swelling.

3.4 Cell encapsulation and culture

In order to study the differentiation of human ADSCs to hepatocytes in a 3D environment, we encapsulated ADSCs in PEG-hydrogel modified with biodegradable PEG-PQ-PEG peptide (described in above) and the cell adhesive peptide PEG-RGDS (detailed above). The hydrogel precursor solution was made by combining, at desired concentrations, PEG-PQ-PEG and PEG-RGDS diluted to desired concentrations with HBS-TEOA and photo initiator solution. In this study, hydrogels of 3%, 5% and 10% PEG-PQ-PEG concentrations were made.

Differentiation of ADSCs into HLCs in this study is influenced by cellular interaction with the growth factors incorporated in the media solutions. In order to check if the growth factors like HGF were able to diffuse through the hydrogel, we also made 5% (~5.6 kPa) hydrogels with HGF encapsulated into the hydrogel crosslink network at photopolymerization by mixing HGF with the polymer precursor solution.

ADSCs cultured and expanded in 2D culture as described in Chapter 2 were trypsinized, centrifuged and then resuspended at a density of 27,000 cells/μl of polymer precursor solution.

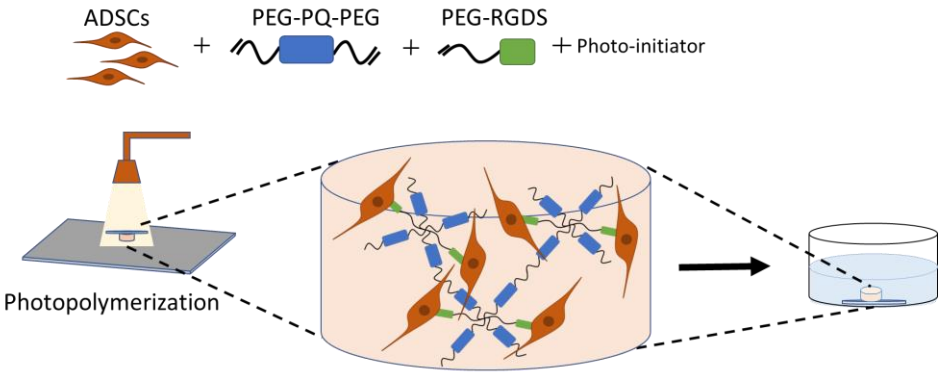

Figure 3.4: Image showing encapsulation of ADSCs in bioactive PEG based hydrogel by photopolymerization reaction. ADSCs are attach via PEG-RGDS peptide in the crosslink network and PEG-PQ-PEG incorporates enzymatically degradable properties to the hydrogel.

2 µl of the cell laden precursor solution was then pipetted between PDMS spacers onto a Sigmacote glass slide (described above), covered with a methacrylate-modified cover slip (described above) and exposed to white light of 150 mW for 35 sec. The gel mounted coverslip was then transferred into a well containing 600 µl of cell endodermal induction media. The cells were then maintained in differentiation protocol as described in chapter 2 above (and detailed in the figure below).

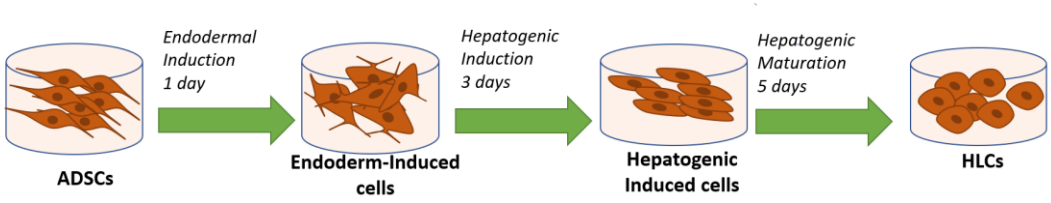

Figure 3.5: Schematic diagram drawn to show the protocol observed for differentiation of ADSCs into HLCs in 3D cell culture. This is according to the conditions in the protocol described and carried out by Xu. et al. (2015) and was adapted for this study to differentiate human ADSCs to functional HLCs.

3.4.1 Immunohistochemistry staining and confocal imaging

For intracellular staining, the cells were fixed with 4% paraformaldehyde for 45 min and then rinsed three times with 1× PBS for 5 min each. The cells were then permeabilized by incubating them with PBS containing 0.5% Triton X-100 (Sigma) for 35 min and then washed four times with PBS. After blocking with 5% donkey serum in PBS overnight, the cells were incubated with primary antibodies diluted in PBS containing 0.05% donkey serum for 48 hr. Primary antibodies, like those used in chapter 2, were; goat anti-ALB (1:150; Bethyl), mouse anti-CD90 (1:200; Biolegend), and rabbit anti-hepatocyte nuclear factor alpha-3 (anti-HNF3β, 1:300; Cell Signaling).

After this stage, the cells were then rinsed three times for 2 hr with PBS + 0.01% Tween20 for the first three washes and the fourth wash with PBS without Tween20. They were then incubated with the appropriate corresponding fluorescently-conjugated secondary antibody (diluted using PBS + 0.05% donkey serum) and left overnight on a rocker at 4^0C in the dark. The corresponding secondary antibodies used were Alexa Fluor 488 conjugated donkey anti-rabbit IgG (1:200, Thermofisher), Alexa Fluor 555 conjugated donkey anti-mouse IgG (1:200, Thermofisher), Alexa Fluor 647 conjugated donkey anti-goat IgG (1:200, Thermofisher).

Cells were then washed with PBS and nuclei were stained by incubation with 4',6-diamidino-2-phenylindole (DAPI; Sigma) for 2 hr and finally washed 3 times for 10 min each with PBS.

Stack images of the hydrogel samples were then imaged using a Zeiss LSM 880 inverted confocal airyscan microscope. Images were taken at 20x objective, 20 μm depth from the hydrogel surface with 2 μm thick sections, 1024 x 1024 pixels, with a line and frame average of 2. The images were then compiled using Image J software.

3.4.2 Hepatic Functional Assays

In order to investigate the properties of the HLCs differentiated from the human ADSCs, we performed assays to test hepatocyte functions like albumin production, urea synthesis and cytochrome P450 (3A4) enzymatic activity. Additionally, these assays were also performed on primary hepatocytes and undifferentiated ADSCs both cultured in 5% hydrogels as our control groups.

3.4.2.1 Albumin Assay

Albumin assays were carried out according to the procedure described in section 2.1.3.1 above. The assays were carried out on conditioned HM medic collected from the wells containing cell laden hydrogels in order to determine if the differentiated HLCs were producing albumin.

3.4.2.2 Cytochrome P450 (3A4) assay

Cytochrome P450 (3A4) assays were carried out according to the procedure described in section 2.1.3.2 above. The fluorescence measured was used to calculate the concentration of produced of CYP generated D-luciferin which is directly proportional to the CYP450 (3A4) enzymatic activity present in the cells.

3.4.2.3 Urea assay

Urea is a main waste product synthesized by the liver from ammonia produced by deamination of amino acids [48]. Urea synthesis is therefore an indicator of hepatocyte functionality [48]. Urea synthesis was quantified using a StanBio Urea Nitrogen quantification assay kit. Samples were from HM media collected on the final day of differentiation. Standard solutions were prepared of 100 μg/mL, 50 μg/mL, 25 μg/mL, 12.5 μg/mL, 6.25 μg/mL, 3.125 μg/mL and 1.562 μg/mL and 0 μg/mL. 10 μl of media samples and 15 μl of standards was added in triplicates to transparent 96 well plates. Blood Urea Nitrogen (BUN) color reagent (containing diacetylmonoxime and thiosemicarbazide) and BUN acid reagent (containing ferric chloride hexahydrate, sulfuric acid and phosphoric acid) were mixed in a ratio of 1:2 respectively. 150 μl of this reagent solution mixture was then added to each of the wells and incubated at 60^0C for 90 min. After the color had developed, the plate reader was used to detect the absorbance at 520 nm. The absorbance was then used to determine to calculate the concentration of urea produced by HLC cells in each gel.

4. Results

4.1 Materials Characterization

4.1.1 Gel Permeation Chromatography

After synthesis of PEG-PQ-PEG and PEG-RGDS peptides from PEG-SVA, the curves below were generated from showing the peaks of the respective peptides generated of relative signal intensity against time.

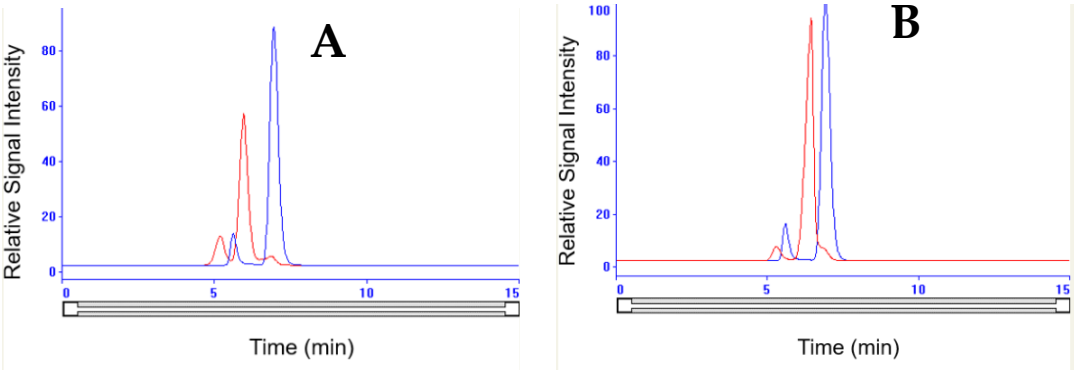

Figure 4.1: Image showing GPC curves for PEG-PQ-PEG (red) (A) and PEG-RGDS (red) (B). PEG-SVA curves are shown in blue in both A and B. The peptides were synthesized with greater than 90% conjugation efficiency.

4.1.2 Cell adhesion study

PEG-RGDS bioactivity was investigated by carrying out a cell adhesion study by seeding MS1 cells onto PEG-RGDS modified PEGDA hydrogels and cell attachment and spreading observed and shown in phase images taken on days 1 and 3 below.

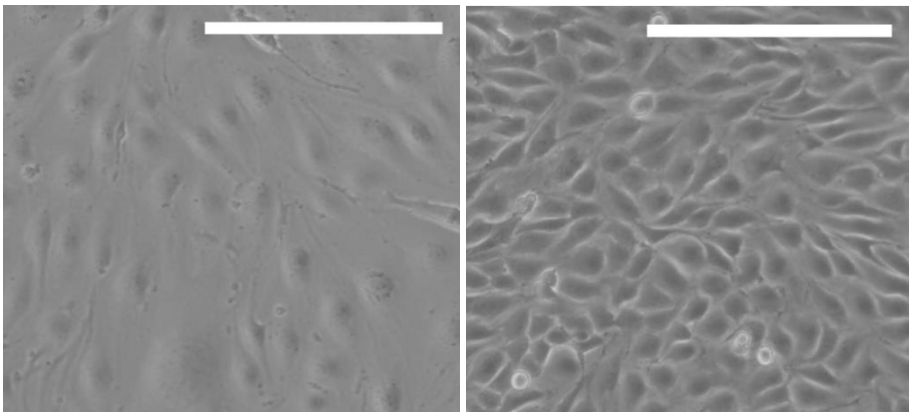

Figure 4.2: Cell adhesion and spreading test to investigate bioactivity of PEG-RGDS. This was achieved by seeding MS1 cells onto PEGDA hydrogel crosslinked with 3.5 mM PEG-RGDS. Images were taken on days 1 and 3 in culture (zoomed images shown above). Attachment of MS1 cells is observed thereby indicating bioactivity of PEG-RGDS for cell attachment and spreading. Scale bar = 200 μm.

4.1.3 Degradation study

The PEG-PQ-PEG hydrogels incubated in collagenase solution were checked every hour to evaluate degradation of the hydrogel. 100% degradation of the hydrogel was observed in 10 hr.

4.1.4 Hydrogel compressive testing

Mechanical properties of the hydrogels indicated a statistically significant increase in the compressive modulus of the hydrogels with increased gel percentage concentration. 3% hydrogels had an average compression modulus of 3.4 ± 1.00 kPa, 5% hydrogels had an average compression modulus of 5.6 ± 2.10 kPa and 10% gels had a compression modulus of 23.3 ± 5.77 kPa.

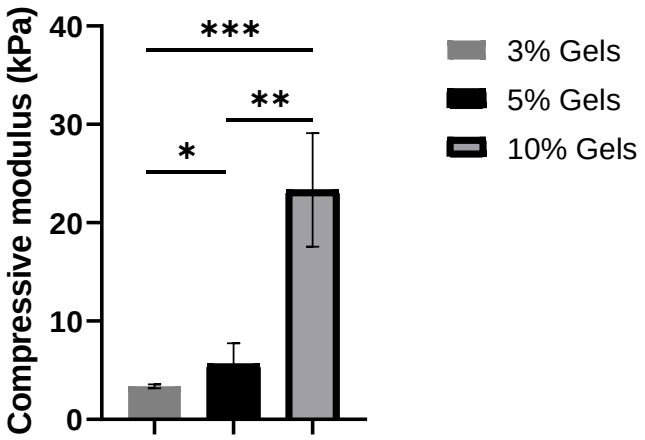

Figure 4.3: Mechanical characterization of PEG-PQ-PEG hydrogels of varying hydrogel percentages. Mechanical testing was performed on 3% (~3.4kPa), 5% (~5.6kPa) and 10% (~23.3 kPa) PEG-PQ-PEG hydrogels resulting in compressive modulus was significantly different between the three groups (p*< 0.05, p< 0.05, p***> 0.05; student t-test).**

4.2 Differentiating ADSCs to HLCs in 2D

Following the differentiation protocol, ADSCs differentiated into HLCs were characterized by visualization techniques (phase contrast and confocal imaging) as well as carrying out hepatocyte functional assays (albumin ELISA and urea assays). The assays were also performed on samples from primary hepatocytes (pHeps) and ADSCs as controls in addition to IHC staining and imaging of primary hepatocytes cultured in 5% gels.

4.2.1 Phase contrast imaging

During the study, there were observed morphological changes in the appearance and shape of the differentiating ADSCs. Hepatocytes were observed to take a less spread appearance than ADSCs as they continued to differentiate.

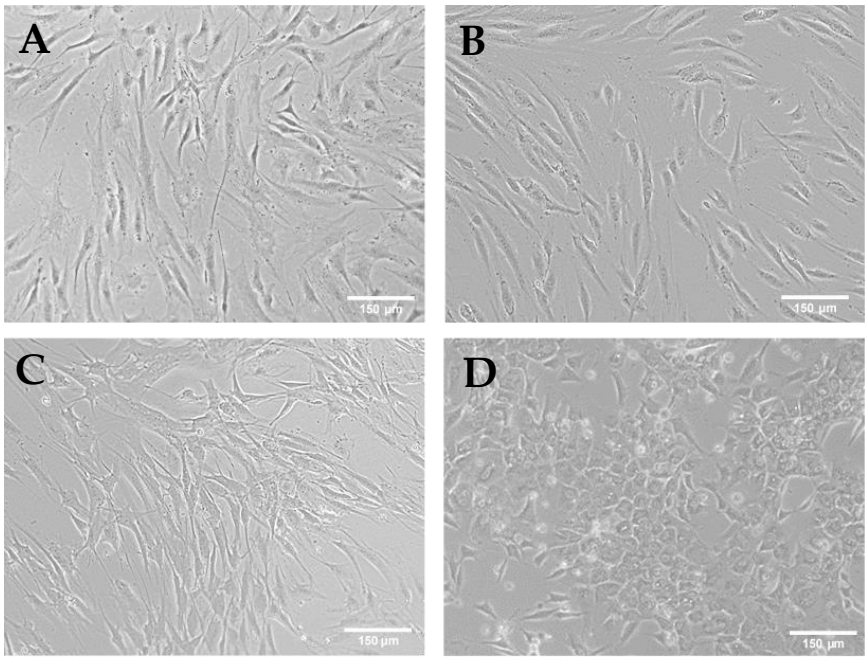

Figure 4.4: The images above show phase contrast images of ADSCs differentiating into HLCs in 2D. Phase images of cells were taken after completion of EI media, HI media, and HM media cycles respectively. A) EI media, B) HI media, C) HM media and D) Primary hepatocytes at day 3 in maintenance media. Scale bars = 150 μm.

4.2.2 Immunohistochemistry staining and confocal imaging

IHC staining revealed presence of albumin and FoxA2/HNF3β, indicating presence of mature hepatocyte markers. However, there was also presence of CD90, our ADSC (stem cell) marker.

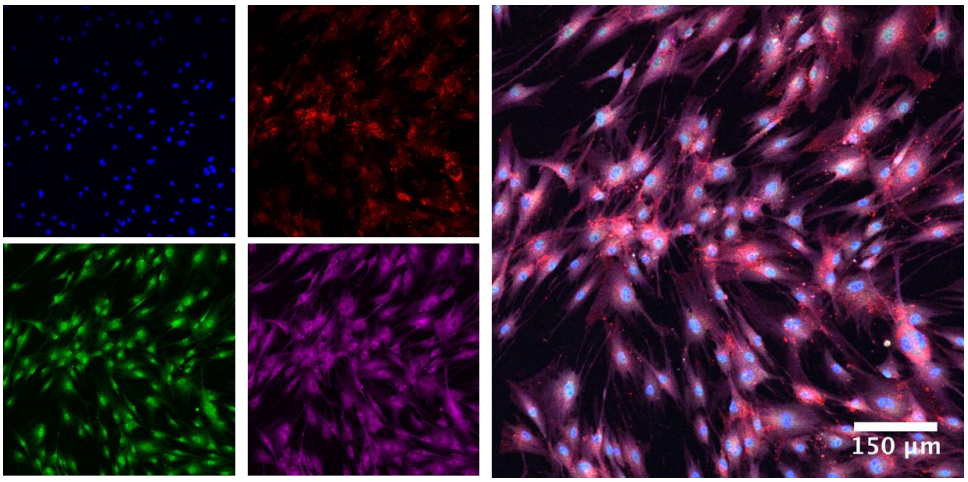

Figure 4.5: Confocal image of HLCs in 2D culture. The HLCs were stained for albumin (magenta) and FoxA2/ HNF3β (green) which are mature hepatocyte markers, as well as for CD90 (red), an ADSC cell marker. Cells were also stained with DAPI (blue) which is a cellular nuclei marker. The 2D cells stained positive for both mature hepatocyte and ADSC markers. Scale bar = 150 µm

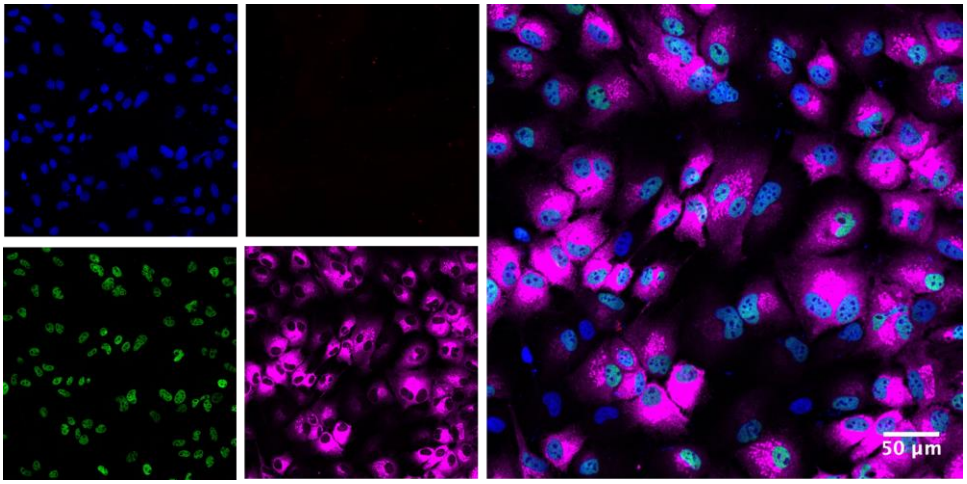

Figure 4.6: Confocal image of primary hepatocytes (pHeps) in 2D culture. The primaries were stained for albumin (magenta) and FoxA2/ HNF3β (green), CD90 (red) and DAPI (blue). They were negative for CD90, the stem cell (ADSC) marker. Scale bar = 50 µm

4.2.3 Albumin quantification ELISA

Quantification of the albumin produced by the HLCs was investigated by carrying out an albumin quantification assay on conditioned HM media samples. The assays revealed an average albumin production of 59.71 ± 18.352 ng/mL in HLCs compared to 68.85 ± 3.330 ng/mL produced by primary hepatocytes of same cell density. Undifferentiated ADSCs on the other hand produced no albumin.

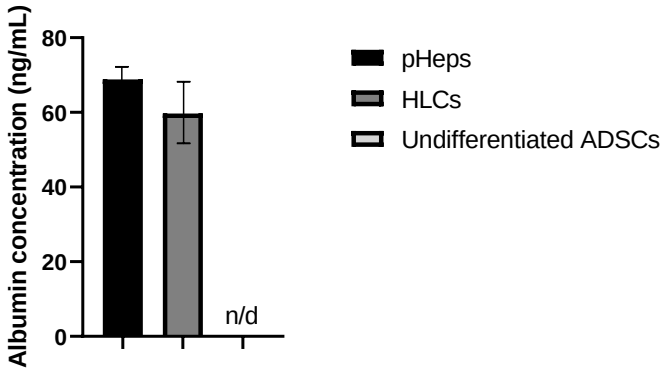

Figure 4.7: Graph showing a comparison of albumin produced by primary hepatocytes, HLCs and undifferentiated ADSCs. No significant difference observed in albumin concentration between HLCs and pHeps ($p > 0.05$; student's t-test).

4.2.4 Urea assay

Urea synthesis was also quantified by carrying out a urea quantification assay which showed an average urea production of approximately 0.24 ± 0.015 μg/mL in HLCs and approximately 0.80 ± 0.18 μg/mL produced by primary hepatocytes while undifferentiated ADSCs had no urea production.

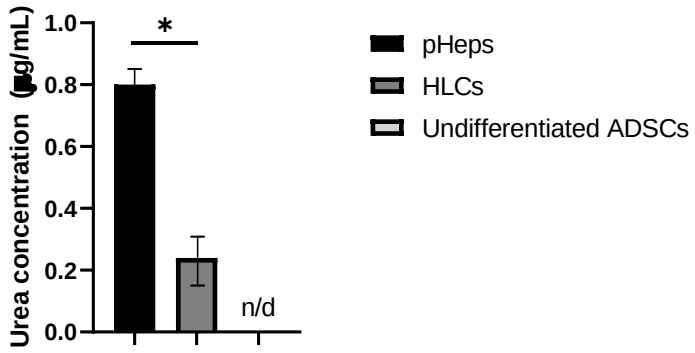

Figure 4.8: Graph showing a comparison in urea concentration produced by primary hepatocytes, HLCs and undifferentiated ADSCs. There was significantly less urea produced by the HLCs compared to pHeps ($p^* < 0.05$; student's t-test).

4.3 Differentiating ADSCs to HLCs in 5% PEG-PQ-PEG hydrogels

Differentiation in 3D was carried out in 5% PEG-PQ-PEG hydrogels. Cell characterization was carried out by phase contrast imaging, IHC staining and confocal imaging. Functional characterization was done by carrying out an albumin ELISA, urea assay on conditioned media as well as a cytochrome P450 (3A4) assay. The results of which are detailed below. Additionally, functional characterization was carried out on primary hepatocytes (pHeps) and undifferentiated ADSCs for comparison.

4.3.1 Phase contrast imaging in 5% (~5.6 kPa) hydrogels

Changes in morphology of the cells was observed while between throughout the differentiation cycle as seen in Figure 4.9 below.

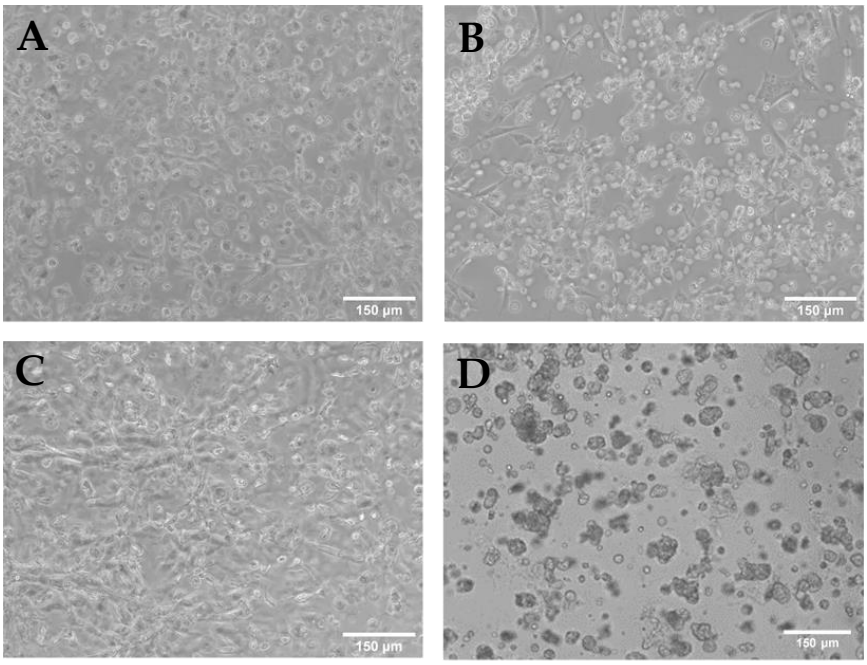

Figure 4.9: The images above (A, B,C) show phase contrast images of ADSCs undergoing differentiation in 5% PEG-PQ-PEG hydrogels (approximately 5.6kPa). A) HLCs on final day of EI media, B) HLCs on final day of HI media, C) HLCs on final day of HM media and D) pHeps on day 3 in hepatocyte maintenance media. Scale bars = 150 μm.

4.3.2 Immunohistochemistry staining and confocal imaging of HLCs encapsulated in 5% (~5.6 kPa) hydrogels

We proceeded to fix and stain the HLCs encapsulated in 5% gels to investigate presence of albumin and FoxA2/ HNF3β markers as the mature hepatocyte markers as well as for CD90 (ADSC marker) and DAPI (cell nuclei marker). Positive markers for albumin and CD90 were observed in HLCs and while only traces of FoxA2/HNF3β were observed as detailed in Figure 4.10 below. pHeps stained for mature hepatocyte markers albumin and FoxA2/ HNF3β but stained negative for CD90, the stem cell (ADSC) marker.

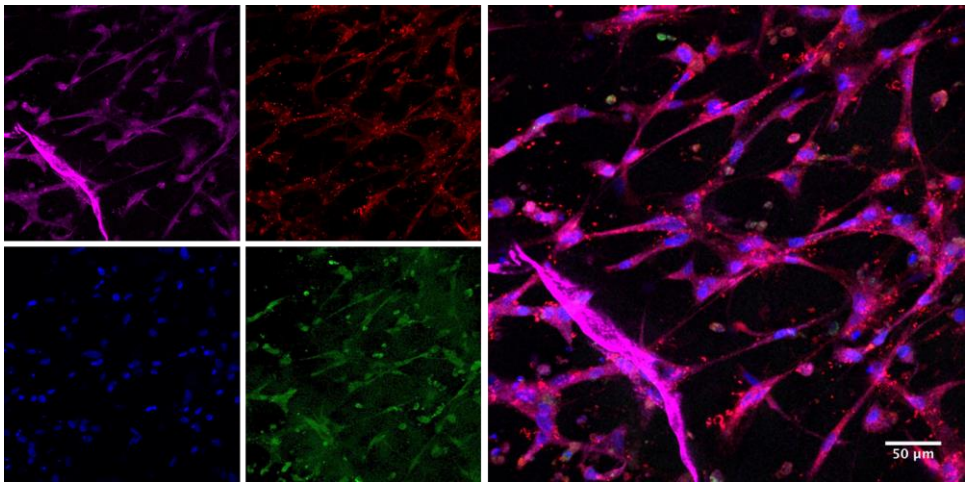

Figure 4.10: Confocal image of HLCs in 3D culture. The cells stained positively for albumin (magenta), traces were of FoxA2/ HNF3β (green) were observed and more strongly for CD90. Cells were also stained with DAPI (blue) which is a cellular nuclei marker. They stained positive for both mature hepatocyte and ADSC markers. Scale bar = 50 µm

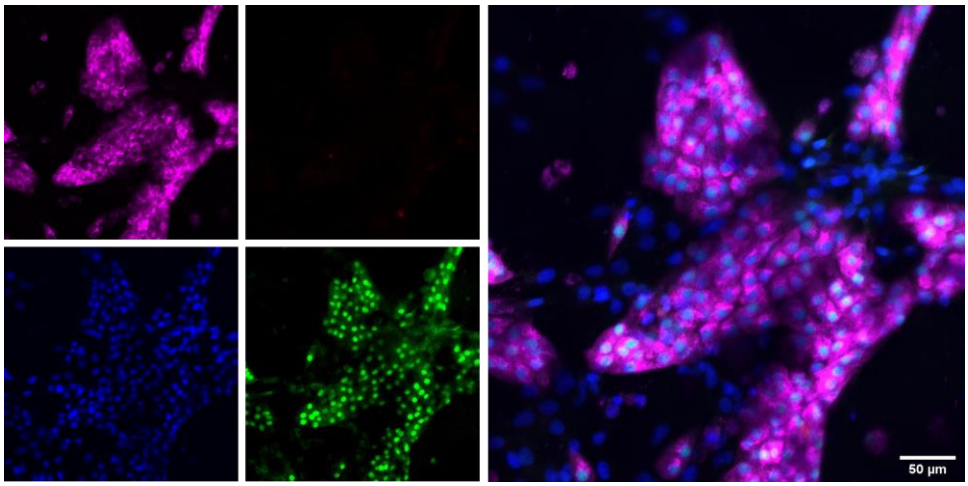

Figure 4.11: Confocal image of primary hepatocytes (pHeps) cultured in 5% hydrogels. The primaries were stained for albumin (magenta) and FoxA2/ HNF3β (green), CD90 (red) and DAPI (blue). They were negative for CD90, the stem cell (ADSC) marker. Scale bar = 50 µm

4.3.3 Albumin quantification ELISA of conditioned media samples from 5% (~5.6 kPa) hydrogels

We went on to quantify the albumin produced by the HLCs in 3D by carrying out an albumin ELISA assay on HM media samples. Albumin present (as observed in IHC staining) was quantified and an average albumin concentration of 54.29 ± 5.640 ng/mL was being produced by HLCs per gel every 24 hr, 89.13 ± 3.433 ng/mL in pHeps per gel every 24 hr and no albumin was produced by undifferentiated ADSCs.

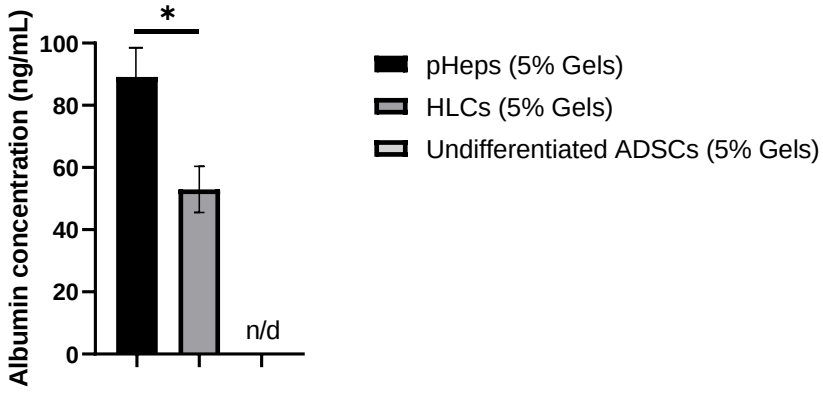

Figure 4.12: Graph showing albumin produced by primary hepatocytes (pHeps), HLCs and undifferentiated ADSCs. All cell groups were encapsulated in 5% (5.6 kPa) hydrogels and there was significantly less albumin produced in the HLCs compared to pHeps ($p^* < 0.05$; student's t-test).

4.3.4 Cytochrome P450 assays for activity in HLCs encapsulated in 5% (~5.6 kPa) hydrogels

CYP450 assays carried out were positive for the presence of cytochrome P450 (CYP3A4) activity. This was determined by quantifying CYP generated D-luciferin as an indicator of CYP3A4 enzyme dependent metabolism. The 5% gels had an average concentration of 1.14 ± 0.149 μM of CYP generated D-luciferin produced per gel every 24

hr, pHeps produced 18.48 14 ± 0.149 μM CYP generated D-luciferin produced per gel every 24 hr as seen below and none was produced by the undifferentiated ADSCs.

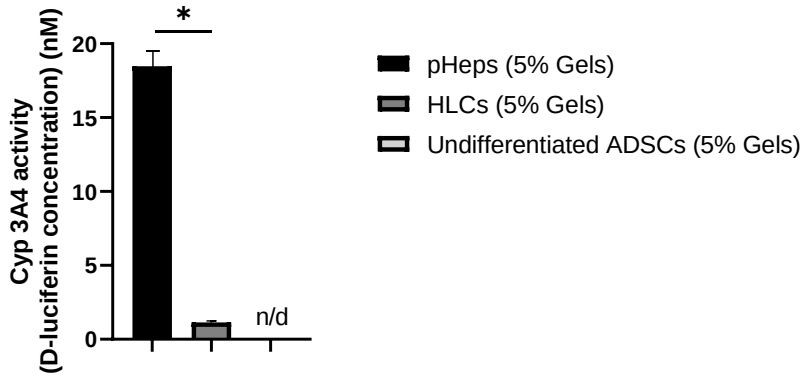

Figure 4.13: D-luciferin concentration produced as an indicator of CYP3A4 activity in pHeps, HLCs and undifferentiated ADSCs. HLCs showed CYP3A4 enzymatic activity although significantly less than in pHeps ($p^* < 0.05$; student's t-test).

4.3.5 Urea assays of conditioned media samples from 5% (~5.6 kPa) hydrogels

Urea production was investigated as an indicator of metabolic properties of the HLCs. A urea assay was carried out on HM media samples and showed an average urea concentration of 0.21 ± 0.019 μg/mL produced by HLCs per gel every 24 hr compared to 1.27 ± 0.103 μg/mL produced by pHeps per gel every 24 hr. Undifferentiated ADSCs produced no urea.

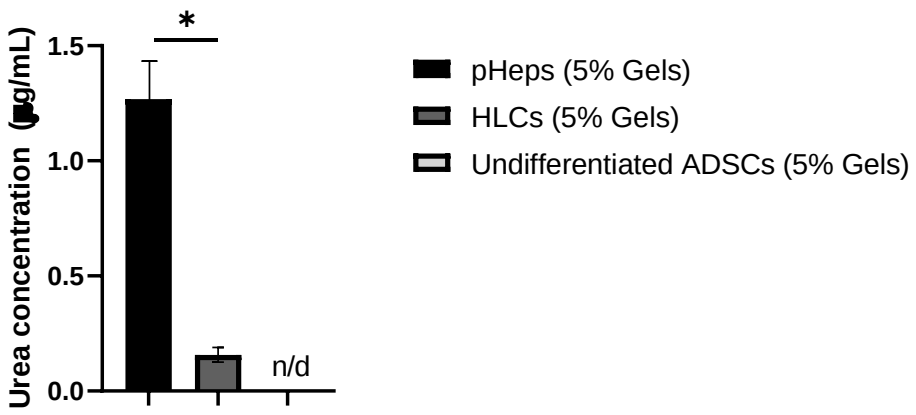

Figure 4.14: Graph showing urea production in HLCs indicating presence of metabolic function. There is a significant difference between HLCs and pHeps groups ($p^* < 0.05$; student's t-test).

4.3.6 Effect of changing gel stiffness on differentiation of ADSCs into HLCs.

In order to optimize differentiation conditions in 3D culture, ADSCs were differentiated to HLCs in hydrogels of different stiffness; 3% (~3.4 kPa), 5% (~5.6 kPa) and 10% (~23.3 kPa) hydrogels. Phase images were taken of the different groups on the final day of differentiation in HM media. Also, an albumin quantification ELISA of conditioned media collected from the 5% and 10% groups was performed to observe the difference in hepatocyte -like function.

There were in cell morphology observed in the hydrogels of different compressive modulus as seen in the phase images below.

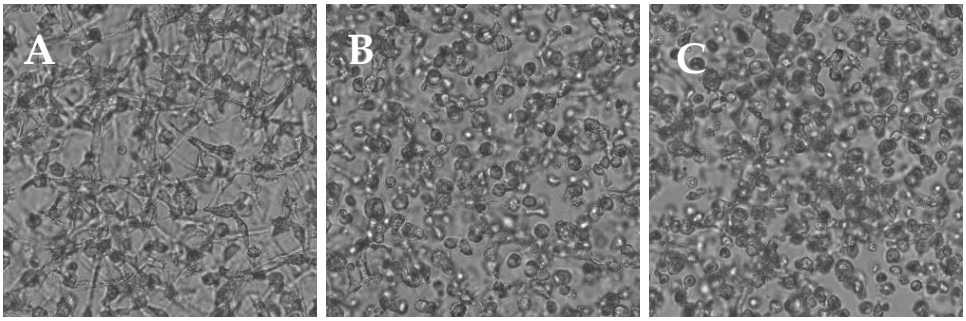

Figure 4.15: The images above show phase contrast images of HLCs in hydrogels of varying stiffness. A) 3% (~3.4 kPa), B) 5% (~5.6 kPa) and C) 10% (~23.3 kPa) PEG-PQ-PEG hydrogels on the final day of HM media. We observe a difference in morphological appearance of the cells in the gels of varying stiffness. Differences in albumin production were observed in the albumin quantification ELISA. HLCs in 10% (23.3 kPa) gels secreted an average of 23.47 ± 1.579 ng/ml per gel every 24 hr. This was significantly less than the albumin concentration of 54.29 ± 5.6 ng/ml produced by HLCs in 5% (~5.6 kPa) gels discussed earlier.

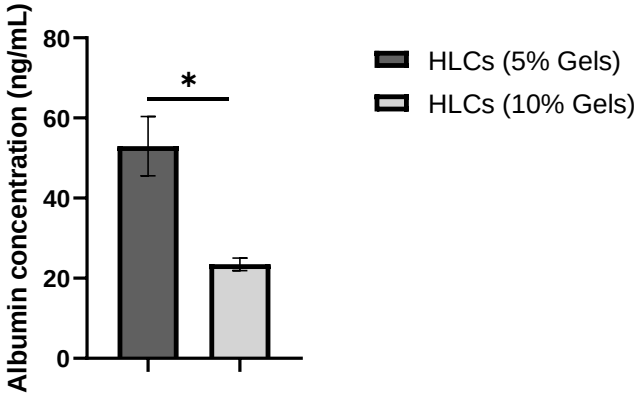

Figure 4.16: The graph shows the average albumin concentration between HLCs in 5% and 10% gels. A significant reduction in albumin production is observed in the 10% gels ($p^* < 0.05$; student's t-test).

4.3.7 Effect of encapsulation of HGF on differentiation of ADSCs into HLCs.

In order to investigate if the growth factors in the differentiation media were diffusing through the hydrogel, HGF (an angiogenic hepatocyte differentiation and growth factor) of 84 kDa in size was encapsulated into the hydrogel. HLC functional properties were determined through an albumin ELISA, urea assay as well as cytochrome P450 activity assay.

Under conditions with HGF encapsulated into the hydrogels, we observed average albumin concentration to 59.57 ± 3.15 ng/ml per gel every 24 hr in hydrogels with encapsulated HGF even though there was no significant difference from 5% gels without encapsulated HGF.

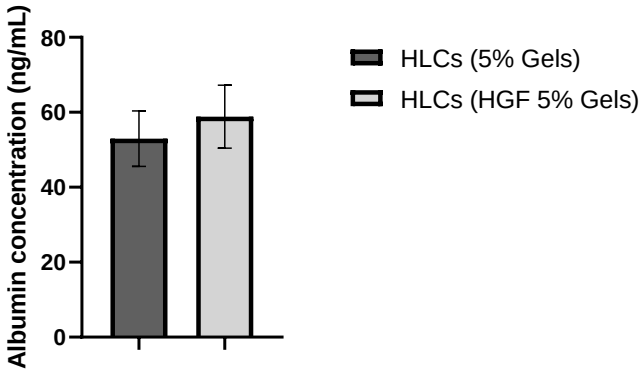

Figure 4.17: The graph shown above shows the average albumin concentration between 5% gels with and without encapsulated HGF. We observe no significant difference in albumin concentration between the two groups ($p > 0.05$; student's t-test).

Presence of cytochrome P450 (3A4) activity was investigated and compared for 5% (~5.6 kPa) gels with and without encapsulated HGF. We observed a concentration of

CYP generated D-luciferin of 1.14 ± 0.149 µM in the 5% (~5.6 kPa) and 0.77 ± 0.204 µM in 5% gels in the gels with HGF incorporated into the hydrogel network. There was a significant reduction in enzymatic activity with the HLCs encapsulated with HGF.

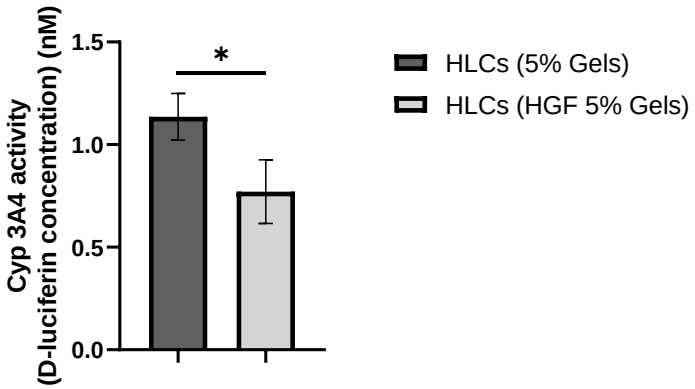

Figure 4.18: Graph comparing CYP3A4 activity between 5% gels with and without encapsulated HGF. There was significantly reduced CYP3A4 activity (p* < 0.05; student's t-test).

IHC staining for CYP3A4 enzyme showed less CYP3A4 enzymes present in HLCs encapsulated with HGF in the hydrogel.

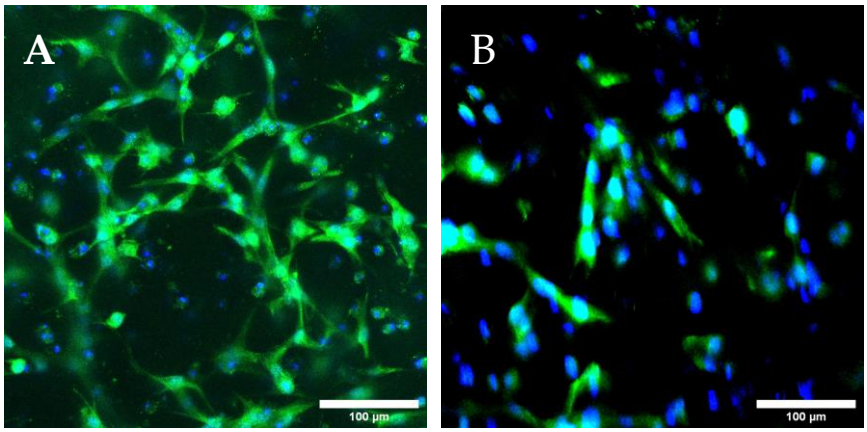

Figure 4.19: HLCs stained for CYP3A4 (green) and DAPI (blue). A) HLCs in 5% gels B) HLCs in hydrogels with encapsulated HGF. Scale bar = 150 µm.

Urea assays carried out to establish the effect of encapsulating HGF on the metabolic activity showed an average urea concentration of 0.16 ± 0.032 μg/ml per gel every 24 hr in 5% gels compared to an average urea concentration of 0.15 ± 0.018 μg/ml per gel every 24 hr produced in the 5% gels with encapsulated HGF. There was no significant difference between the groups.

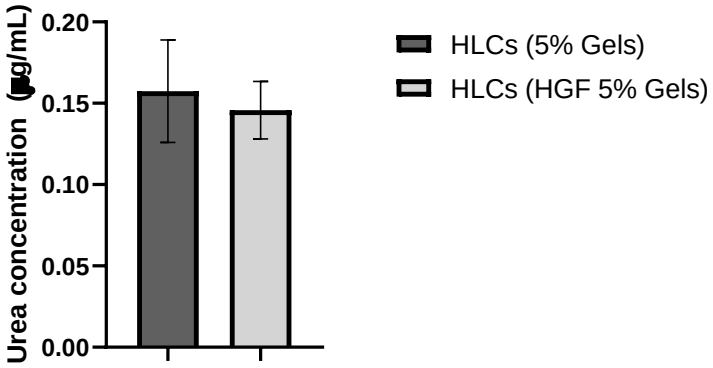

Figure 4.20: The graph shows the average urea produced between 5% gels with and without encapsulated HGF. We observe no significant difference in urea concentration between the two groups ($p > 0.05$; student's t-test).

5. Discussion

The goal of this study was to be able to differentiate human ADSCs into functional HLCs. This is in order to provide a source of cells that can carry out hepatocyte functions for application in bioartificial liver support devices that are currently being used to 'bridge' acute and acute-on-chronic liver patients to liver transplants or allow liver regeneration and recovery [36, 43]. This study was carried out by adapting the protocol used by Xu et al. [48] in their work of differentiating rat ADSCs to functional HLCs and using the same protocol to culture and induce differentiation of human ADSCs to HLCs in 2D culture and 3D culture. Achieving the first study aim was carried out by culturing and differentiating human ADSCs into HLCs in 2D culture as described in chapter 2.

In both 2D and 3D culture, we observed changes in the morphology of the differentiating cells after each cycle of media change as seen in Figure 4.4 and Figure 4.9 above indicative of differentiation process taking place. Upon fixing and staining the HLCs for mature hepatocyte marker albumin, we observed that both the 2D and 3D samples were differentiating into cells with positive albumin markers. However, cells in 2D culture showed more presence of FoxA2/ HNF3β compared to the traces seen in the 3D samples. This is probably due to incomplete maturation of immature hepatocytes into mature hepatocytes. in 3D culture. There was also presence of CD90 showing that some of the ADSCs cultured did not differentiate and remained stem cells. This could be

because human ADSCs require different time exposure to the induction media and growth factors compared to the rat ADSCs differentiated by Xu et al. Similarly, encapsulated ADSCs might also require longer exposure time to induction media in order to account for the 3D nature of the hydrogel and therefore allowing diffusion of induction media for differentiation.

Positive presence of mature hepatocyte markers after IHC staining in some HLCs shows that the induction media and growth factors do indeed induce differentiation of human ADSCs into HLCs. Albumin ELISA assays of HM media samples showed production of albumin and thus indicative of hepatocyte-like function. HLCs produced an average albumin concentration of 59.7 ± 18.35 ng/ml which was not significantly different from pHeps that produced an average of 68.85 ± 3.330 ng/mL of albumin. HLCs had albumin production functions within the range of primary hepatocytes and this indicated presence of protein synthesis functions in the HLCs. HLCs encapsulated in 5% (~5.6 kPa) also possessed protein synthesis (albumin production) properties with an average albumin concentration of 54.29 ± 5.6 ng/ml produced by HLCs per well. This however was significantly less than average albumin concentration of 89.13 ± 3.433 ng/mL produced by primary hepatocytes encapsulated in 5% gels. This is because not all the cells differentiated successfully (as also seen by presence of ADSC markers after IHC staining) into HLCs and therefore albumin was being produced by only a fraction of the

encapsulated cells. Incomplete differentiation suggests the need for more optimized incubation time of ADSCs in the different induction media.

Urea and cytochrome P450 (3A4) assays were carried out to further establish metabolic and enzymatic properties of the HLCs generated by differentiation from human ADSCs. Urea production was present in HLCs cultured both in 2D and 3D and the urea quantification assays which showed an average urea production of approximately 0.24 ± 0.015 μg/ml by HLCs per gel every 24 hr compared to a significantly greater amount produced by pHeps of approximately 0.80 ± 0.18 μg/mL per gel every 24 hr. Similarly, in the 5% (~5.6 kPa) gels, HLCs produced an average urea concentration of 0.21 ± 0.019 μg/mL per gel every 24 hr compared to 1.27 ± 0.103 μg/mL produced by pHeps per gel every 24 hr. In the same way, in HLCs, we observed significantly less CYP3A4 generated D-luciferin of approximately 1.14 ± 0.149 μM per gel every 24 hr compared to pHeps that produced an average of 18.48 14 ± 0.149 μM CYP generated D-luciferin per gel every 24 hr. Even with high concentrations of albumin produced, there is less metabolic and enzymatic function observed in HLCs compared to pHeps. This could be because differentiation could have resulted into formation of both hepatocytes and biliary cells. Biliary cells and hepatocytes have been shown to have the same differentiation pathway (Figure 5.1 below) from stem cells until final differentiation from liver progenitor hepatoblasts [42, 48]. Biliary cells also produce some albumin [61] even though in significantly smaller amounts than primary

hepatocytes. They however have no metabolic and enzymatic functions characteristic of primary hepatocytes. It is therefore possible that during differentiation, some biliary cells were formed instead of hepatocytes. However, this can only be confirmed by further studies carried out and staining for biliary cell markers.

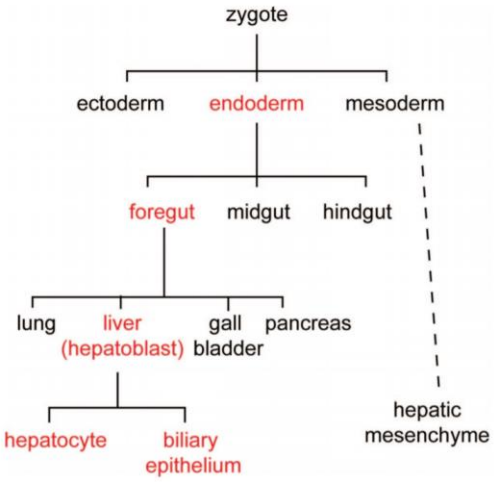

Figure 5.1: Pathway for differentiation of hepatocytes from stem cells [62].

Mechanical characterization of the PEG-PQ-PEG hydrogels revealed the compressive modulus of 3%, 5% and 10% gels to be approximately 3.4 kPa, 5.6 kPa and 23.3 kPa respectively (Figure 4.3). The 3D microenvironment of stem cells has been shown to have a bearing on the differentiation pathways of the cells [59]. Similarly, in this study, we observed that a variation in mechanical strength of the PEG-PQ-PEG hydrogels had an impact on the morphological appearance of the HLCs (Figure 4.15). Additionally, we observed a significant reduction in albumin concentrations between the 5% (~5.6 kPa) and 10% (~23.3 kPa) which produced an average albumin concentration of 23.47 ± 1.579 ng/ml per gel. The significant reduction in albumin

production could be because the 10% gels (~23.3 kPa) were significantly stiffer than the liver whose compressive modulus is between 2.6 - 6.2 kPa [63] compared to 5% (~5.6 kPa) gels which are within this range.

Since the differentiation protocol had only been previously used in 2D culture and the growth factors to induce differentiation to HLCs were all present in media, we were concerned about possible difficulty in diffusion of the constituent growth factors in media into the hydrogel to interact with the cells. As such, we investigated albumin and cytochrome P450 activity in 5% (~5.6 kPa) hydrogels with HGF (of 84 kDa) was incorporated in the crosslinking hydrogel network. This is because it is a key constituent of HI and HM media as a key hepatocyte differentiation and maturation growth factor [50]. From the results, we observed no significant difference in albumin or urea production between the two groups of 5% (5.6 kPa) gels with and without HGF incorporated in the gel network. This means that we expect that growth factors were able to adequately diffuse through the hydrogel and induce differentiation of HLCs from human ADSCs. We did however observe a significant difference in CYP3A4 activity with a reduction in CYP activity observed in the samples with encapsulated HGF. This is because HGF is a strong angiogenic growth factor and studies have shown that HGF down regulates expression of CYP450 isoenzymes in human hepatocytes in primary culture and improves albumin production [64].

6. Conclusion and future work

Presence of positive IHC staining of mature hepatocyte markers, and functional properties of albumin and urea production as well as cytochrome P450 activity are all indicators that differentiation of human ADSCs to HLCs is possible in 2D and in bioactive PEG-PQ-PEG hydrogel following thee protocol described in the earlier chapters. Unfortunately, this alone is not enough to confirm reliable and efficient differentiation and therefore further optimization of the differentiation protocol is necessary. This would include determining the ideal time required for the cells in each media cycle tailored especially for 3D culture. Other factors like cell density, concentrations of constituent growth factors could be investigated for further. The change in hepatocyte function further emphasizes that differentiation is influenced by environmental cues like mechanical properties or introduction of biochemical cues [51]. The effects were observed through significant difference in the albumin concentrations with increased gel stiffness and reduced cytochrome P450 enzymatic activity with encapsulation of HGF.

Repetitive and efficient differentiation of human ADSCs into functional HLCs in bioactive PEG-PQ-PEG hydrogels would provide a cell source for liver support devices that overcomes the shortcomings of most other available cell sources [13]. The ADSCs would be an abundant supply of large quantities of cells that can be easily obtained and therefore overcoming the constraints faced by bioartificial liver support devices [37].

7. References

1. Kumar, A., A. Tripathi, and S. Jain, *Extracorporeal bioartificial liver for treating acute liver diseases.* J Extra Corpor Technol, 2011. **43**(4): p. 195-206.

2. Lonza. *Importance of Primary Hepatocytes in early ADME-Tox studies | Lonza*. 2019; Available from: https://bioscience.lonza.com/lonza_bs/CH/en/early-admetox-studies.

3. *How does the liver work?* 2016.

4. Kim, W.R.L., J. R. Smith, J. M. Skeans, M. A. Schladt, D. P. Edwards, E. B. Harper, A. M. Wainright, J. L. Snyder, J. J. Israni, A. K. Kasiske, B. L., *Liver.* American Journal of Transplantation, 2016.

5. Phua, J. and K.H. Lee, *Liver support devices.* Curr Opin Crit Care, 2008. **14**(2): p. 208-15.

6. Michalopoulos, G.K., *Liver Regeneration.* J Cell Physiol, 2007. **213**(2): p. 286-300.

7. Clavien, P.-A., et al., *Strategies for Safer Liver Surgery and Partial Liver Transplantation.* http://dx.doi.org/10.1056/NEJMra065156, 2009.

8. Murphy, N., *An update in acute liver failure: when to transplant and the role of liver support devices.* Clin Med (Lond), 2006. **6**(1): p. 40-6.

9. Hyperarts, R.M.-. *End-stage Liver Disease (ESLD)*. 2019.

10. Fox, I.J., *Hepatocyte Transplantation.* Gastroenterol Hepatol (N Y), 2014. **10**(9): p. 594-6.

11. Pless, G., *Artificial and bioartificial liver support.* Organogenesis, 2007. **3**(1): p. 20-4.

12. Lee, K.C., V. Stadlbauer, and R. Jalan, *Extracorporeal liver support devices for listed patients.* Liver Transpl, 2016. **22**(6): p. 839-48.

13. Stevens, K., et al., *Hepatic Tissue Engineering*, in *Principles of Tissue Engineering*. 2014, Academic Press: Science Direct. p. 951-986.

14. Mokdad, A.A., et al., *Liver cirrhosis mortality in 187 countries between 1980 and 2010: a systematic analysis.* BMC Medicine, 2014. **12**.

15. Prevention, C.f.D.C.a., *QuickStats: Death Rates for Chronic Liver Disease and Cirrhosis, by Sex and Age Group — National Vital Statistics System, United States, 2000 and 2015 | MMWR*, C.f.D.C.a. Prevention, Editor. 2017, Centers for Disease Control and Prevention: MMWR Morbility & Mortality Weekly Report.

16. Bernal, W., G. Auzinger, and A. Dhawan, *Acute Liver failure.* The Lancet, 2010. **276**(9736): p. 190-201.

17. Lee, W.M., *Acute liver failure in the United States.* Semin Liver Dis, 2003. **23**(3): p. 217-26.

18. Williams, R., *Classification, etiology, and considerations of outcome in acute liver failure.* Semin Liver Dis, 1996. **16**(4): p. 343-8.

19. Gill, R.Q. and R.K. Sterling, *Acute liver failure.* J Clin Gastroenterol, 2001. **33**(3): p. 191-8.

20. Lee, W.M., et al., *Acute liver failure: Summary of a workshop.* Hepatology, 2008. **47**(4): p. 1401-15.

21. Hay, J.E., *Acute Liver Failure.* Curr Treat Options Gastroenterol, 2004. **7**(6): p. 459-468.

22. Leise, M.D., J.J. Poterucha, and J.A. Talwalkar, *Drug-induced liver injury.* Mayo Clin Proc, 2014. **89**(1): p. 95-106.

23. Williams, R., S.W. Schalm, and J.G. O'Grady, *Acute liver failure: redefining the syndromes.* The Lancet, 1993. **342**(8866).

24. Shakil, A.O., et al., *Acute liver failure: clinical features, outcome analysis, and applicability of prognostic criteria.* Liver Transpl, 2000. **6**(2): p. 163-9.

25. Kim, T.Y. and D.J. Kim, *Acute-on-chronic liver failure.* Clin Mol Hepatol, 2013. **19**(4): p. 349-59.

26. Asrani, S.K. and J.G. O'Leary, *Acute-on-Chronic Liver Failure.* Clin Liver Dis, 2014. **18**(3): p. 561-74.

27. Arroyo, V. and R. Jalan, *Acute-on-Chronic Liver Failure: Definition, Diagnosis, and Clinical Characteristics.* Semin Liver Dis, 2016. **36**(2): p. 109-16.

28. Hernaez, R., et al., *Acute-on-chronic liver failure: an update.* 2017.

29. Ibars, E.P., et al., *Hepatocyte transplantation program: Lessons learned and future strategies.* World J Gastroenterol, 2016. **22**(2): p. 874-86.

30. Castell, J.V., et al., *Hepatocyte cell lines: their use, scope and limitations in drug metabolism studies.* Expert Opin Drug Metab Toxicol, 2006. **2**(2): p. 183-212.

31. Tanimizu, N. and T. Mitaka, *Which is better source for functional hepatocytes?* Stem Cell Investig, 2017. **4**.

32. Adham, M., *Extracorporeal liver support: waiting for the deciding vote.* ASAIO J, 2003. **49**(6): p. 621-32.

33. Peterson, R.G. and L.N. Peterson, *Cleansing the blood. Hemodialysis, peritoneal dialysis, exchange transfusion, charcoal hemoperfusion, forced diuresis.* Pediatr Clin North Am, 1986. **33**(3): p. 675-89.

34. Kaplan, A.A. and M. Epstein, *Extracorporeal blood purification in the management of patients with hepatic failure.* Semin Nephrol, 1997. **17**(6): p. 576-82.

35. Pascher, A., et al., *Extracorporeal liver perfusion as hepatic assist in acute liver failure: a review of world experience.* Xenotransplantation, 2002. **9**(5): p. 309-24.

36. Nandhini A. J. Lakshmi, K.K., *Liver support devices: Bridge to transplant or recovery.* Indian Journal of Respiratory Care, 2017. **6**(2): p. 807-812.

37. Baquerizo, A., R. Bañares, and F. Saliba, *Current Clinical Status of the Extracorporeal Liver Support Devices*, in *Transplantation of the Liver*. 2015. p. 1463-1487.

38. Court, F.G., et al., *Bioartificial liver support devices: historical perspectives.* ANZ J Surg, 2003. **73**(9): p. 739-48.

39. Park, J.K. and D.H. Lee, *Bioartificial liver systems: current status and future perspective.* J Biosci Bioeng, 2005. **99**(4): p. 311-9.

40. Fourneau, I. and P. Yap, *Bioartificial liver support: recent advances.* Acta Chir Belg, 2000. **100**(6): p. 276-8.

41. Palakkan, A.A., et al., *Liver tissue engineering and cell sources: issues and challenges.* Liver Int, 2013. **33**(5): p. 666-76.

42. Sauer, V., et al., *Induced pluripotent stem cells as a source of hepatocytes.* Curr Pathobiol Rep, 2014. **2**(1): p. 11-20.

43. van de Kerkhove, M.P., et al., *Bridging a patient with acute liver failure to liver transplantation by the AMC-bioartificial liver.* Cell Transplant, 2003. **12**(6): p. 563-8.

44. Borowiak, M., et al., *Small molecules efficiently direct endodermal differentiation of mouse and human embryonic stem cells.* Cell Stem Cell, 2009. **4**(4): p. 348-58.

45. Hass, R., et al., *Different populations and sources of human mesenchymal stem cells (MSC): A comparison of adult and neonatal tissue-derived MSC.* Cell Communication and Signaling, 2011. **9**(1): p. 12.

46. Banas, A., et al., *Adipose tissue-derived mesenchymal stem cells as a source of human hepatocytes.* Hepatology, 2007. **46**(1): p. 219-28.

47. Locke, M., J. Windsor, and P.R. Dunbar, *Human adipose-derived stem cells: isolation, characterization and applications in surgery.* ANZ J Surg, 2009. **79**(4): p. 235-44.

48. Xu, F., et al., *Rapid and high-efficiency generation of mature functional hepatocyte-like cells from adipose-derived stem cells by a three-step protocol.* Stem Cell Res Ther, 2015. **6**: p. 193.

49. Engert, S., et al., *Wnt/beta-catenin signalling regulates Sox17 expression and is essential for organizer and endoderm formation in the mouse.* Development, 2013. **140**(15): p. 3128-38.

50. Siller, R., et al., *Small-Molecule-Driven Hepatocyte Differentiation of Human Pluripotent Stem Cells.* Stem Cell Reports, 2015. **4**(5): p. 939-52.

51. Tibbitt, M.W. and K.S. Anseth, *Hydrogels as Extracellular Matrix Mimics for 3D Cell Culture.* Biotechnol Bioeng, 2009. **103**(4): p. 655-63.

52. Moore, E.M. and J.L. West, *Bioactive Poly(ethylene Glycol) Acrylate Hydrogels for Regenerative Engineering.* Regenerative Engineering and Translational Medicine, 2018: p. 1-13.

53. Edmondson, R., et al., *Three-Dimensional Cell Culture Systems and Their Applications in Drug Discovery and Cell-Based Biosensors.* Assay Drug Dev Technol, 2014. **12**(4): p. 207-18.

54. Ahmed, E.M., *Hydrogel: Preparation, characterization, and applications: A review.* Journal of Advanced Research, 2015. **6**(2): p. 105-121.

55. Lee, J.H. and H.W. Kim, *Emerging properties of hydrogels in tissue engineering.* J Tissue Eng, 2018. **9**.

56. Zhu, J., *Bioactive modification of poly(ethylene glycol) hydrogels for tissue engineering.* Biomaterials, 2010. **31**(17): p. 4639-56.

57. Zustiak, S.P. and J.B. Leach, *Hydrolytically Degradable Poly(Ethylene Glycol) Hydrogel Scaffolds with Tunable Degradation and Mechanical Properties.* Biomacromolecules, 2010. **11**(5): p. 1348-1357.

58. Nguyen, K.T. and J.L. West, *Photopolymerizable hydrogels for tissue engineering applications.* Biomaterials, 2002. **23**(22): p. 4307-14.

59. Ovadia, E.M., D.W. Colby, and A.M. Kloxin, *Designing well-defined photopolymerized synthetic matrices for three-dimensional culture and differentiation of induced pluripotent stem cells.* Biomater Sci, 2018. **6**(6): p. 1358-1370.

60. Peters, E.B., et al., *Poly(ethylene glycol) Hydrogel Scaffolds Containing Cell-Adhesive and Protease-Sensitive Peptides Support Microvessel Formation by Endothelial Progenitor Cells.* Cell Mol Bioeng, 2016. **9**(1): p. 38-54.

61. Germain, L., M.J. Blouin, and N. Marceau, *Biliary Epithelial and Hepatocytic Cell Lineage Relationships in Embryonic Rat Liver as Determined by the Differential Expression of Cytokeratins, α-Fetoprotein, Albumin, and Cell Surface-exposed Components | Cancer Research.* Cancer Research, 1988. **48**: p. 4909-4918.

62. RBPAonline. *Gastrointestinal Tract Liver Development Embryology #164289400683 – Ectoderm Mesoderm Endoderm Derivatives Flow Chart (+42 More files) | RBPAonline.com*. 2019; Available from: http://rbpaonline.com/ectoderm-mesoderm-endoderm-derivatives-flow-chart/gastrointestinal-tract-liver-development-embryology/.

63. Suh, C.H., et al., *Determination of Normal Hepatic Elasticity by Using Real-time Shear-wave Elastography.* Radiology, 2014.

64. Donato, M.T., et al., *Human hepatocyte growth factor down-regulates the expression of cytochrome P450 isozymes in human hepatocytes in primary culture.* J Pharmacol Exp Ther, 1998. **284**(2): p. 760-7.